Synthesis of chemical tools to study the immune system

Graaff, M.J. van de

Chapter 2

Conditionally controlled TLR2/6 ligands[1,2]

Introduction

Toll-like receptor 2 (TLR 2) is localized on the surface plasma membrane. Like most TLRs, it is expressed predominantly in dendritic cells and macrophages.[3] Agonist binding and heterodimerization with either TLR1 or TLR6 initiates downstream signaling transduction.[4,5] The acylation pattern of the ligand dictates which dimer is stabilized: Pam_3CSK_4 (Figure **1**C) engages the TLR2/1 signaling pathway[6], whereas Pam_2CSK_4 engages the TLR2/6 signaling pathway.[4,5]

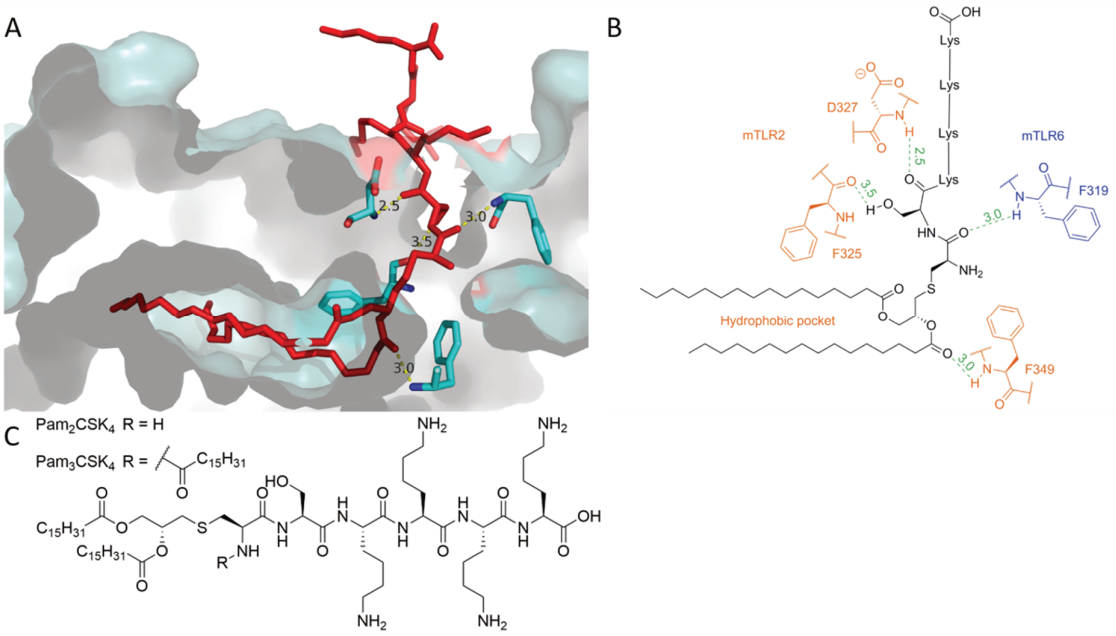

Figure 1. Ligand binding of Pam_2CSK_4 to TLR2/6 A) Surface rendering of the crystal structure of Pam_2CSK_4-bound TLR2/6[4]. Key interacting residues are highlighted with putative hydrogen bond lengths (Å). B) Schematic representation of A). Depicted in orange are TLR2 residues, depicted in blue a TLR6 residue. Green dashed lines represent potential hydrogen bonds with calculated distances noted in Ångström units of length. The four C-terminal lysine residues of the ligand have no interaction with the TLR2/6 complex. The two palmitoyl tails fit inside a hydrophobic pocket present on TLR2. C) Structures of Pam_2CSK_4 and Pam_3CSK_4.

Crystal structure analysis of the TLR2/1-Pam_3CSK_4 complex revealed that two palmitoyl tails of Pam_3CSK_4 are anchored within a hydrophobic pocket inside the TLR2 ectodomain.[5] The third palmitoyl tail, present on the N-terminus of the ligand, bridges the gap between TLR2 and TLR1 and is anchored within a hydrophobic tunnel of the TLR1 ectodomain, facilitating stabilization of the dimer. When considering the TLR2/6 dimer however, the hydrophobic tunnel in TLR6

(structurally similar to TLR1) is blocked by the side-chains of two phenylalanine residues, precluding anchoring of the palmitoyl tail and thus binding with Pam_3CSK_4.[4] Instead, another phenylalanine residue (F319, Figure **1**B) is located on the dimerization interface, capable of forming a hydrogen bond with the cysteine-serine amide bond in the ligand. For this interaction to occur any acylation on the N-terminus of the ligand is excluded, thus Pam_2CSK_4 gains selectivity for TLR2/6 whereas Pam_3CSK_4 is selective for TLR2/1.

Recently, it became evident that not only the ligand structure can dictate signaling outcome of TLRs, but also the cellular localization in the cell where the receptor is activated.[7,8] This was first exemplified in the activation of TLR4, signaling events of which induce the production of pro-inflammatory cytokines and type I interferons (IFN-I).[9] Presence of inhibitors that block endocytosis prevented the production of IFN-I, but not of pro-inflammatory cytokines.[7,8] The signaling pathways are differentially engaged through recruitment of specific adaptor proteins on the cytosolic domain of TLR dimers. It is now believed the spatially distinct pathways are engaged in a sequential manner, meaning the adaptor molecule responsible for pro-inflammatory cytokine production is displaced by recruitment of the adaptor protein responsible for IFN-I production as the TLR4-ligand complex translocates to endosomes.

The signaling platforms present on cell surface-residing TLR2 resemble that of TLR4, both recruiting TIRAP and MyD88 to activate NF-κB. However, different adaptors are recruited in endosomally localized TLRs. Yet not much is known about the bifurcation of TLR2 signaling, in part due to the lack of chemical tools in the immunologist's repertoire. Until now, endocytosis inhibitors were the prime choice of reagent to probe for spatiotemporal effects, but these can perturb other cellular processes to such extent that experimental outcome cannot be entirely conclusive.[10]

A ligand's activity needs to be spatially and temporally controlled in order to accurately decouple spatiotemporal complexity in TLR activation. The aim was therefore to synthesize TLR2/6 ligands that were able to be activated on demand, with the ultimate goal of decoupling endosomal activation from cell surface TLR activation. Mancini *et al.* found that protecting the N-terminal amine of Pam_2CSK_4 with an *ortho*-nitrobenzyl (*o*-NB) derived biologically compatible protecting group – or 'cage' – precludes TLR2/6 dimerization, but not binding to TLR2.[11] This enables pretreatment of cells with the caged ligand, priming all the TLR2s for dimerization. Removal of the cage by applying light as an external trigger restored dimerization with TLR6 thus achieving temporal control over TLR activation. Spatial control is limited by the accuracy with which the apparatus can irradiate the sample, the scattering of the UV-photons as well as the minimum irradiation time (as BMDCs rapidly move outside the irradiation area within the minimum timeframe needed to photo-uncage[12]).

Although these limitations can be overcome with two-photon irradiation, where volumes as small as 1 femtoliter can be irradiated with near-IR light[13], the aim was to explore the use of chemo-labile cages to selectively activate TLRs in endosomes. To this end, a suitable cage would have to 1) be stable, as TLRs are highly sensitive for small amounts of free ligand due to a positive feedback loop exerted by the signaling cascade, 2) uncage quickly, as transcription of the first cytokines start

within 15 minutes of activation[14,15], and 3) be spatial controllable in its uncaging: its uncaging reagents have to be directable specifically to endosomes.

One such cage was discovered in 2008 by Prof. Joseph Fox. The Fox lab discovered that *trans*-cyclooctenes (TCOs) ligate with tetrazines with a rate of 2000 $M^{-1}s^{-1}$, enabling fast and quantitative reactions at low concentrations (Figure 2).[16] In 2013, Marc Robillard and co-workers modified the TCO to include a hydroxyl functionality at the 2-position that would allow it to function as a bio-compatible release reaction.[17]

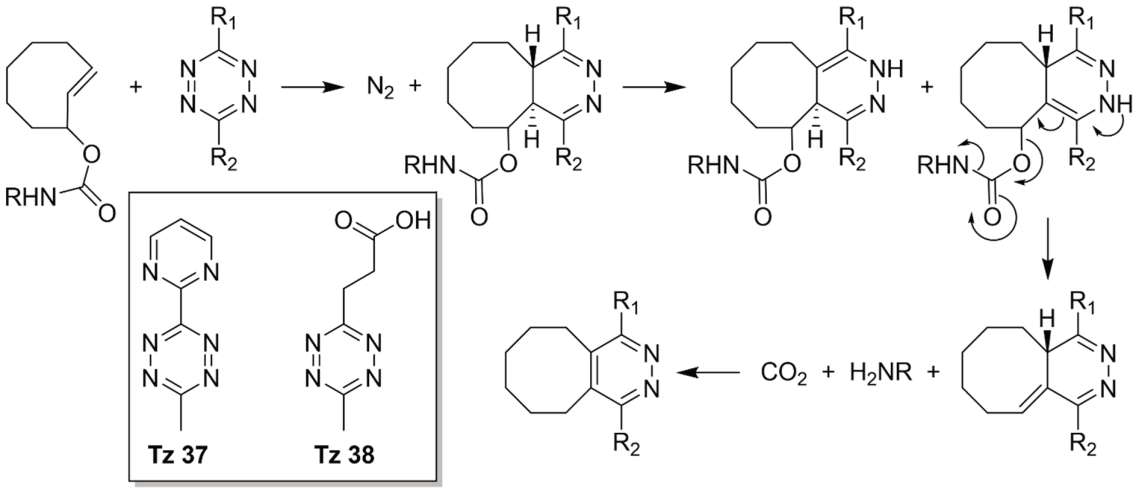

Figure 2. Ligation of a tetrazine and 2-alkoxy-TCO. Inverse electron demand Diels-Alder ligation of the tetrazine with the TCO leads to expulsion of nitrogen and formation of the adduct. Tautomerization leads to two structural isomers of which one is primed for consequent elimination. Structures of tetrazines employed in this chapter are given.

Amines that are coupled to this hydroxyl through a carbamylation are released upon ligation of tetrazine and subsequent tautomerization. As the axial isomer of the hydroxyl is more reactive and less sterically hindered towards elimination, isolation of this isomer comes with a rate constant of $7.9 * 10^4\ M^{-1}s^{-1}$ in water at 20 °C. This pioneering work initiated the possibility of bio-orthogonally uncaging quantitatively, in a short timeframe at low concentrations with a reagent that appears non-toxic, even *in vivo.*[18,19] The tetrazine reaction partner can be modified to alter the reaction kinetics[20], or to restrict cell permeability by incorporating ionic substituents or by immobilization onto a surface. For a fast ligation one R-substituent needs to have an electron-withdrawing character, whereas the elimination step is heavily reliant on the second R-substituent to be non-electron-withdrawing. Building on this knowledge, tetrazine 37 (Figure 2) was developed by the group of Peng Chen, to exert the highest uncaging activity in living cells.[20] Since then Sarris and co-workers have developed even faster tetrazines, carrying aminoethyl substituents at the para-position.[21]

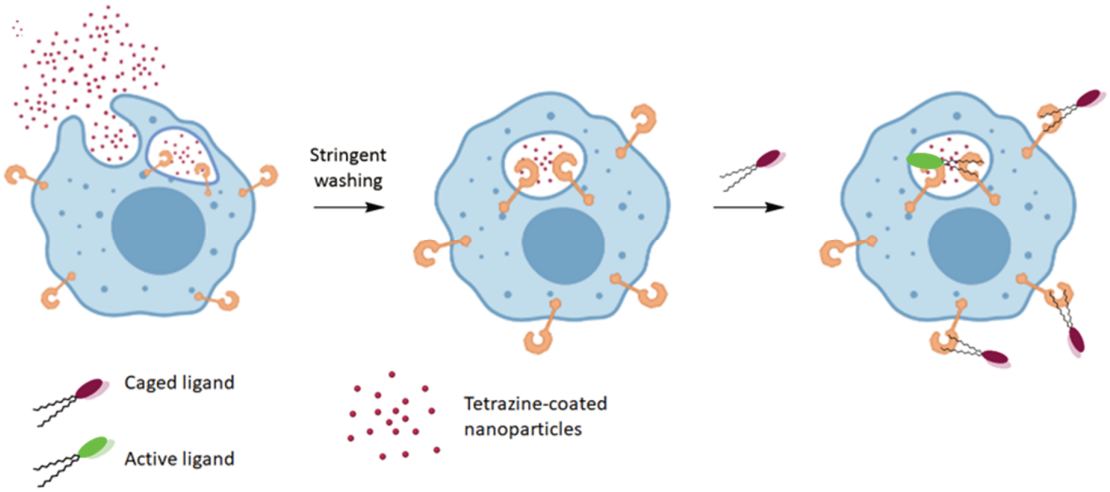

Figure 3. A strategy to activate intracellular TLRs. First the cells are treated with tetrazine-coated nanoparticles which are taken up through phago- and endocytic pathways. After a stringent washing procedure, the cells are treated with TCO-caged TLR-ligand. Liberation of the ligand from its cage should now be prevalent in intracellular vesicles as opposed to the extracellular environment.

It was envisaged that the localization of tetrazines in endosomes by immobilization of tetrazine **38** onto nano-sized amine-coated beads could yield endosome-selective deprotection agents. These beads would be endocytosed by the DC or macrophage, after which a stringent washing procedure would remove all remaining extracellular beads. Treatment with the caged ligand would then result in accumulation of free ligand only inside endosomes carrying the tetrazine beads. Alternatively, were the tetrazine to be sufficiently derivatized with electron-withdrawing groups, the reaction rate of elimination drops to zero whilst maintaining proper ligation kinetics. It was envisaged that decoration of such a tetrazine with cell permeability-restricting entities would lead to a valuable tool to inactivate TCO-bearing species on the cell surface. In other words, treatment of cells that are primed with caged ligand with such a tetrazine would result in permanently inactive *surface-residing only* TLR-ligand complexes. A second treatment with a *cell-permeable* tetrazine would then uncage all endosomally localized ligands. These are two hypothetic examples with which the TCO-tetrazine reaction can be used to spatially control TLR activity. In the context of TLR2/6, the lipopeptide Pam_2CSK_4 had to be functionalized with axial 2-TCO on the N-terminal amine. *Cis*-cyclooctene does not ligate with tetrazine at a significant reaction rate, but the similarity in the chemophysical properties makes it a useful control compound. Thus, both TCO- and CCO-bearing ligands were synthesized in parallel.

Results and Discussion

The synthesis of Pam_2CSK_4 and its protected derivatives focused on obtaining chirally pure R-Pam_2Cys, as the S-epimer of Pam_2CSK_4 is significantly less active.[22] This building block was obtained on gram-scale starting from relatively cheap starting materials as illustrated in Scheme 1.[23]

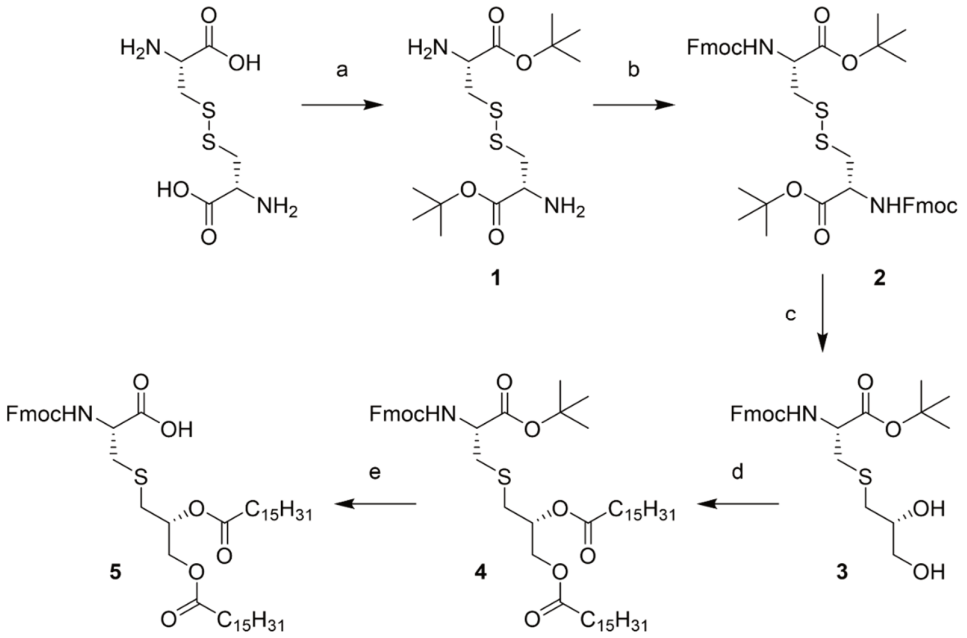

Scheme 1. Synthesis of chirally pure Fmoc-Pam_2Cys-OH (R-epimer) building block on multi-gram scale. **a)** t-butyl acetate, 70% $HClO_4$, r.t., 75 hrs, qt.; **b)** Fmoc-OSu, N-methyl morpholine, THF, r.t., 2 hrs, 68%; **c)** (i) Zn powder (10 µm), 93:6:1 MeOH:37% HCl (aq.):98% H_2SO_4, r.t., 15 min (ii) R-(+)-glycidol, r.t., 72 hrs, 78%; **d)** Palmitic acid, diisopropylcarbodiimide, DMAP, DCM, r.t., o.n., 95%; e) TFA, r.t., 1 hr, qt.

L-Cystine was protected as a *tert*-butyl ester in a transesterification reaction catalyzed by perchloric acid after which a fluorenylmethyl oxycarbonyl was installed on both amines. The disulfide bridge was reduced using activated zinc powder in an acidic environment after which enantiopure R-glycidol was added to alkylate the liberated thiol in a one-pot procedure. The zinc powder was observed to aggregate 10 minutes after the addition of the acidic mixture which corresponded with completion of the disulfide reduction. Interestingly, when the zinc powder was removed at this stage, addition of R-glycidol did not result in any product formation, whilst robust product formation was observed in the flask that did contain zinc. This indicated an – as yet unidentified – functional role of the zinc in the alkylation step. Esterification with palmitic acid, di-isopropylcarbodiimide and a catalytic amount of DMAP resulted in di-protected compound **4**. Removal of the *tert*-butyl group with neat TFA yielded Fmoc-Pam_2Cys-OH **5** in a 50% overall yield on a multi-gram scale.

A facile method of synthesizing (caged) Pam_2CSK_4 derivatives is by making use of Fmoc-based solid-phase peptide synthesis (SPPS) as the C→N synthesis allows the introduction of the TCO in the final step. The relatively labile TCO therefore did not have to endure multiple coupling and deprotection steps. However, global deprotection often involves highly concentrated mixtures of TFA, observed to have the potential to isomerize or even eliminate 2-oxo-*trans*-cyclooctenes. Global deprotection strategies involving basic conditions may in turn hydrolyze the palmitoyl esters present on the cysteine residue. Therefore, a strategy was chosen where global deprotection can be carried out in dilute TFA using monomethyltrityl (MMTrt) protecting groups and the highly acid labile S-Ac linker.

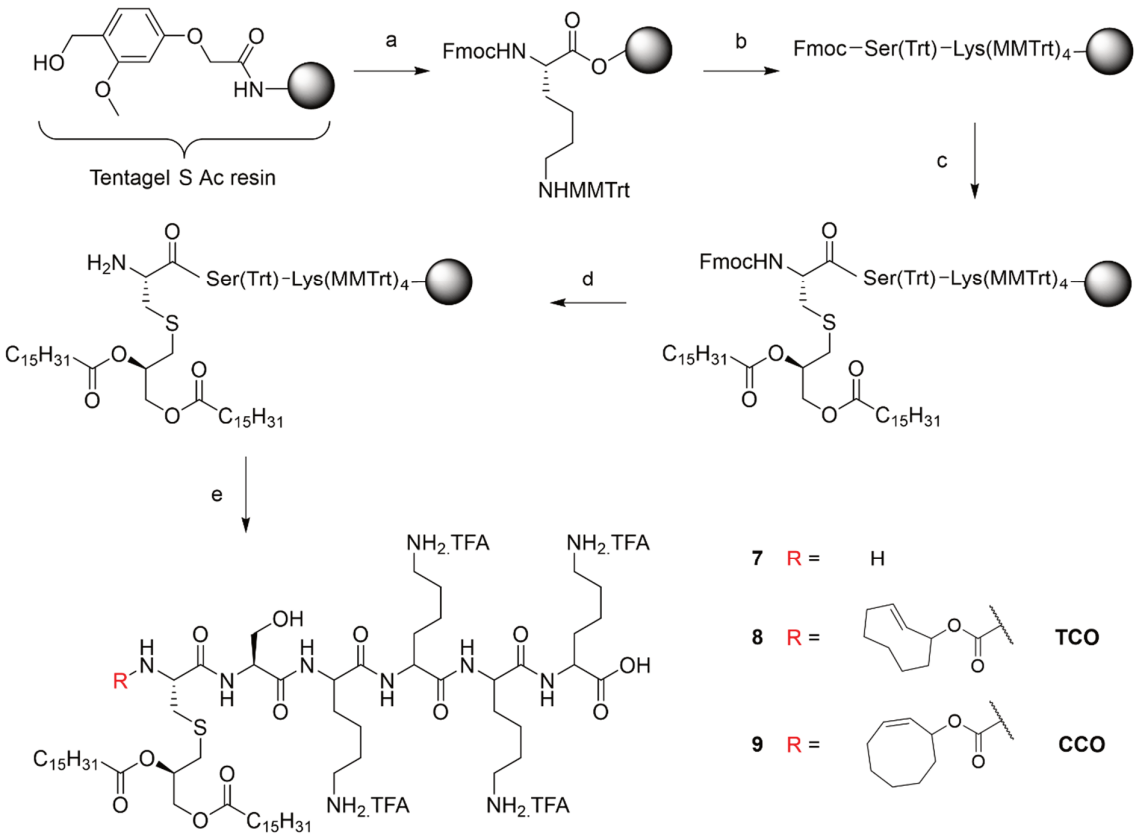

Scheme 2. Synthesis of TCO/CCO-caged P_2CSK_4. Reagents and conditions: **a)** Fmoc-Lys(MMTrt), diisopropylcarbo-diimide, DMAP, r.t., o.n.; **b)** (i) 20% piperidine in DMF, r.t., 10 min (3x) (ii) amino acid (0.6 M in DMF), HCTU (0.6 M in DMF), DiPEA (0.6 M in DMF), r.t., 2 hrs (iii) 5% acetic anhydride in DMF (containing 0.1 M DiPEA), r.t., 10 min; **c)** (i) 20% piperidine in DMF, r.t., 10 min (3x) (ii) HCTU (0.6 M in DMF), **5** (0.6 M in DMF), DiPEA (0.6 M in DMF), r.t., 2 hrs (iii) 5% acetic anhydride in DMF (containing 0.1 M DiPEA), r.t., 10 min; **d)** 20% piperidine in DMF, r.t., 10 min (3x); **e)** Compound **7**: 20% TFA, 2.5% TIS and 2.5% H_2O in DCM, r.t., 1 hr; Compound **8**: (i) TCO-OSu, DiPEA, DMF, r.t., o.n. (ii) 5% TFA, 2.5% TIS and 2.5% H_2O in DCM, r.t., 1 hr; Compound **9**: (i) CCO-OSu, DiPEA, DMF, r.t., o.n. (ii) 5% TFA, 2.5% TIS and 2.5% H_2O in DCM, r.t., 1 hr.

Using standard Fmoc-based SPPS coupling/deprotection cycles (HCTU / piperidine in DMF), H_2N-Pam_2CS(Trt)(K(MMTrt))$_4$ was obtained on resin (Scheme **2**). The free amine was treated either with axial TCO-OSu or CCO-OSu and DiPEA. Global deprotection with 5% TFA in DCM appeared sufficient to cleave the product from the resin, although due to the extreme lipophilicity of the product standard precipitation methods failed. Cooling the precipitation solvent to -20°C and centrifuging at 4°C for several hours yielded some precipitation, but not in a consistent manner. Direct injection of the crude deprotection mixture (reconstituted in DMSO after evaporation) on HPLC seemed the only viable strategy to consistently afford product isolation, albeit in poor (4% overall) yield. HPLC using 0.1% TFA as a mobile phase modifier is preferentially avoided due to the aforementioned acidic lability of 2-oxo-TCO. However, basic HPLC buffers such as ammonium carbonate proved impractical, as the deprotonated lysine amines

affected the polarity in favor of hydrophobic interactions to such degree that no suitable gradient system was found that yielded pure product. The ionization in the HPLC-MS was also affected to such degree that no ion threshold count could be reached to initiate sample collection. Therefore, TCO-Pam_2CSK_4 was purified on HPLC using 0.1% TFA as a mobile phase modifier. Care was taken when concentrating the collected fractions, as prolonged concentration at elevated temperatures was observed to lead to isomerization or hydrolysis of the TCO, resulting in contamination of free ligand or permanently silenced ligand in the final product.

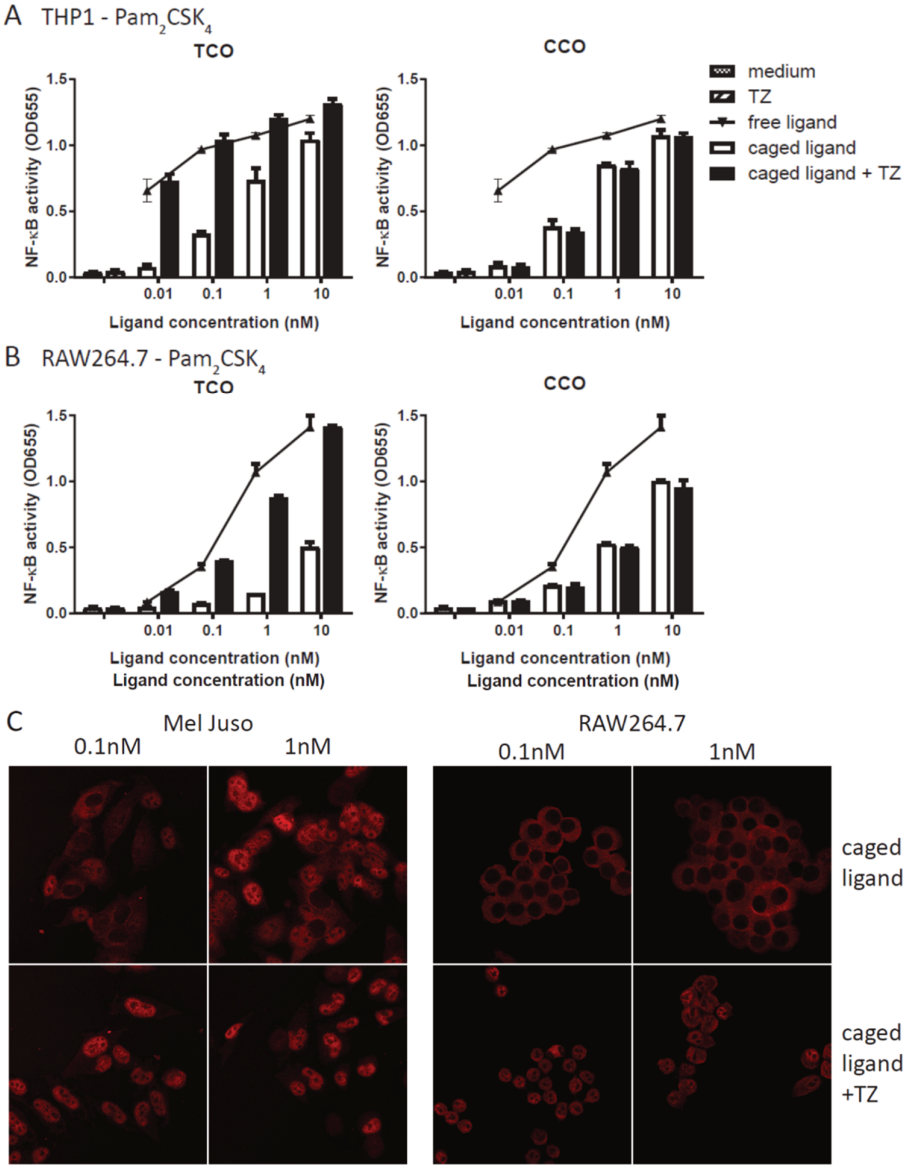

Figure 4. Chemical uncaging of Pam_2CSK_4-TCO induces NF-κB activation both in human THP1-Dual **(A)** or murine RAW-Blue **(B)** cells were pre-incubated with the indicated ligands for 45 min. Fresh medium +/- tetrazine was added and after 24hrs NF-κB activity was measured in the culture supernatant using a SEAP colorimetric assay. **C)** Cells were pre-incubated with Pam_2CSK_4-TCO for 45 min. Cells were washed and fresh medium +/- tetrazine was added. After 30 min cells were fixed and stained for p65 (NFκB). Experiments were carried out by Timo Oosenbrug (LUMC).

The distinctness of the activation profile between human and mouse TLR2/6 activation was of primary interest. Therefore, the uncaging reaction of compounds **8** and **9** was tested on both a human cell line (THP1-Dual) and murine (RAW264.7) cell line (Figure **4**). THP1-Dual is a monocyte cell line containing two inducible reporter constructs: the NF-kB-pathway can be monitored by activity of Secreted Embryonic Alkaline Phosphatase (SEAP) and simultaneously the IRF-pathway can be monitored by the activity of secreted luciferase (Lucia).

RAW-Blue is a mouse macrophage cell line with a SEAP reporter construct inducible by NF-kB, expressing all TLR's except TLR5. The cells were incubated either with compounds **8** or **9** for 45 minutes prior to the addition of a 10 μM solution of tetrazine **37** (Figure **2**), or no addition of tetrazine. SEAP levels were measured in the culture supernatant as a measure of NF-kB activity. The level of NF-kB activity for the CCO-caged compounds is independent of addition of tetrazine **37**, exhibiting only residual activity of the caged ligand. The TCO-caged ligand does react with the tetrazine, resulting in an increase of NF-kB activity at every concentration range for both cell types. Interestingly, the RAW macrophages require a 100-fold higher concentration of ligand to achieve the same level of activation when compared to the THP1 cells. The nuclear translocation of NF-kB was visualized using p65-RFP expressing Mel Juso (human) and RAW264.7 cells under confocal microscopy (Figure **4**C). The p65-RFP is a fluorescently labeled subunit of the NF-kB complex which translocates to the cell nucleus upon TLR2/6 activation. The murine cells exhibited several concentrations in which a favorable window of uncaging existed: activating almost every cell which was inactive prior the addition of tetrazine **37**. Surprisingly, no concentration exhibiting a favorable window of uncaging existed when Mel Juso cells were employed.

It was hypothesized that the *cis*-/*trans*-cyclooctene either undergo hydrophobic-hydrophobic interactions with a hydrophobic patch present on hTLR6 but not mTLR6, or that the cages suffer from insufficient bulk to counteract the dimerization of TLR2/6. Since no crystal structure of hTLR2/hTLR6 is available, it was chosen to append either a small or a large hydrophilic group from the existing cage that would probe which of these effects were causing background activity. For the small-to-medium appendages, linkers containing alcohols, sulfonates or monodisperse ethylene glycols were chosen. For the large appendage, the small protein ubiquitin was chosen. Ubiquitin is an 8.6 kDa water soluble, accessible and thermally stable protein containing seven lysine residues, useable as sites of conjugation.[24]

Introducing the hydrophilic appendage in TCO-caged Pam_2CSK_4 was facilitated by using the recently published bis-functionalized TCO-$(OSu)_2$ (compound **14**, Scheme **3**).[25] Amines react regioselectively with the NHS-carbonate prior to reacting with the sterically hindered NHS-ester.

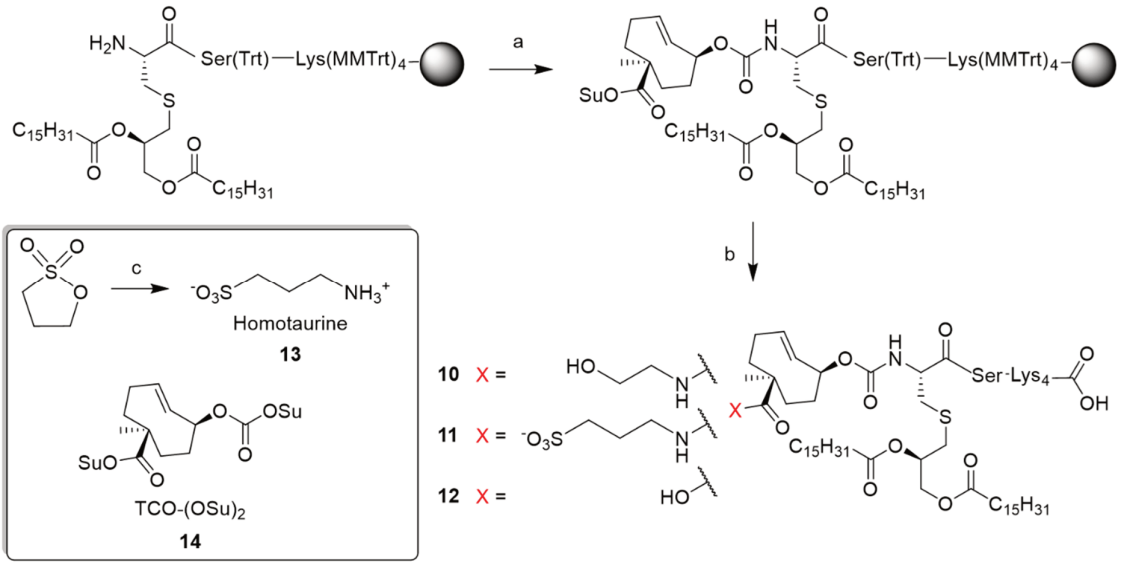

Scheme 3. Synthesis of TCO-caged P_2CSK_4 bearing hydrophilic linkers on the cyclooctene. Reagents and conditions: **a)** TCO-$(OSu)_2$, DiPEA, DMF, r.t., o.n. **b)** (i) Compound **10**: ethanolamine, DCM, r.t., o.n. (ii) 5% TFA, 2.5% TIS, 2.5% H_2O, DCM, r.t., 30 min; Compounds **11** and **12**: (i) homotaurine **13**, DiPEA, DMSO, r.t., o.n. (ii) 5% TFA, 2.5% TIS, 2.5% H_2O, DCM, r.t., 30 min. **c)** 7N methanolic ammonia, 0°C → r.t.

Three hydrophilic derivatives of TCO-P_2CSK_4 were synthesized on-resin by first reacting the free amine P_2CSK_4 with the bis-functionalized TCO-$(OSu)_2$ reagent **14** (Scheme **3**). When LC-MS indicated complete conversion, the resin was washed and treated with either ethanolamine or homotaurine. Homotaurine itself was synthesized by treating 1,3-propanesultone with methanolic ammonia and subsequent precipitation in diethylether. Conjugation with homotaurine resulted in a mixture of partially hydrolyzed NHS-ester→carboxylic acid (**12**) and product **11** in a 1:1 ratio, whereas conjugation with ethanolamine resulted in quantitative conversion to the respective product. Unfortunately, HPLC purification proved unsuccessful in isolating either of the three products. Also, no formation of product was observed when conjugation with ubiquitin was attempted. This was, however, unsurprising as conjugating a large molecule to an activated ester immobilized on solid phase often suffers from extremely low coupling efficiencies. This construct therefore warranted a solution-phase coupling strategy.

Solution-phase couplings require the lysine side chains to be deprotected after conjugation has taken place. The use of the TCO added the restraint that acid- or base-labile protecting groups could not be used. This quickly leads to a complex synthetic route accompanied with complex purification methods. Therefore, it was decided to substitute the C-terminal tetralysine motif for a triethylene glycol (TEG) linker. This adaptation was postulated to minimally influence the activity of the ligand as the tetralysine moiety does not interact with the mTLR2/mTLR6 dimer in the published crystal structure, and conjugates have been described previously employing this motif.[26] Moreover, the two linkers share the same length with heteroatoms (O for TEG and N for Lys_4) in the same position in the carbon backbone. With the lysine primary amines now excluded, the serine alcohol is the only other functional group bearing nucleophilic character. The N-terminal cysteine

amine should outcompete the serine alcohol in terms of nucleophilicity, thus omitting any protecting group usage when the TCO/CCO is introduced in the ligand in a solution-phase coupling strategy.

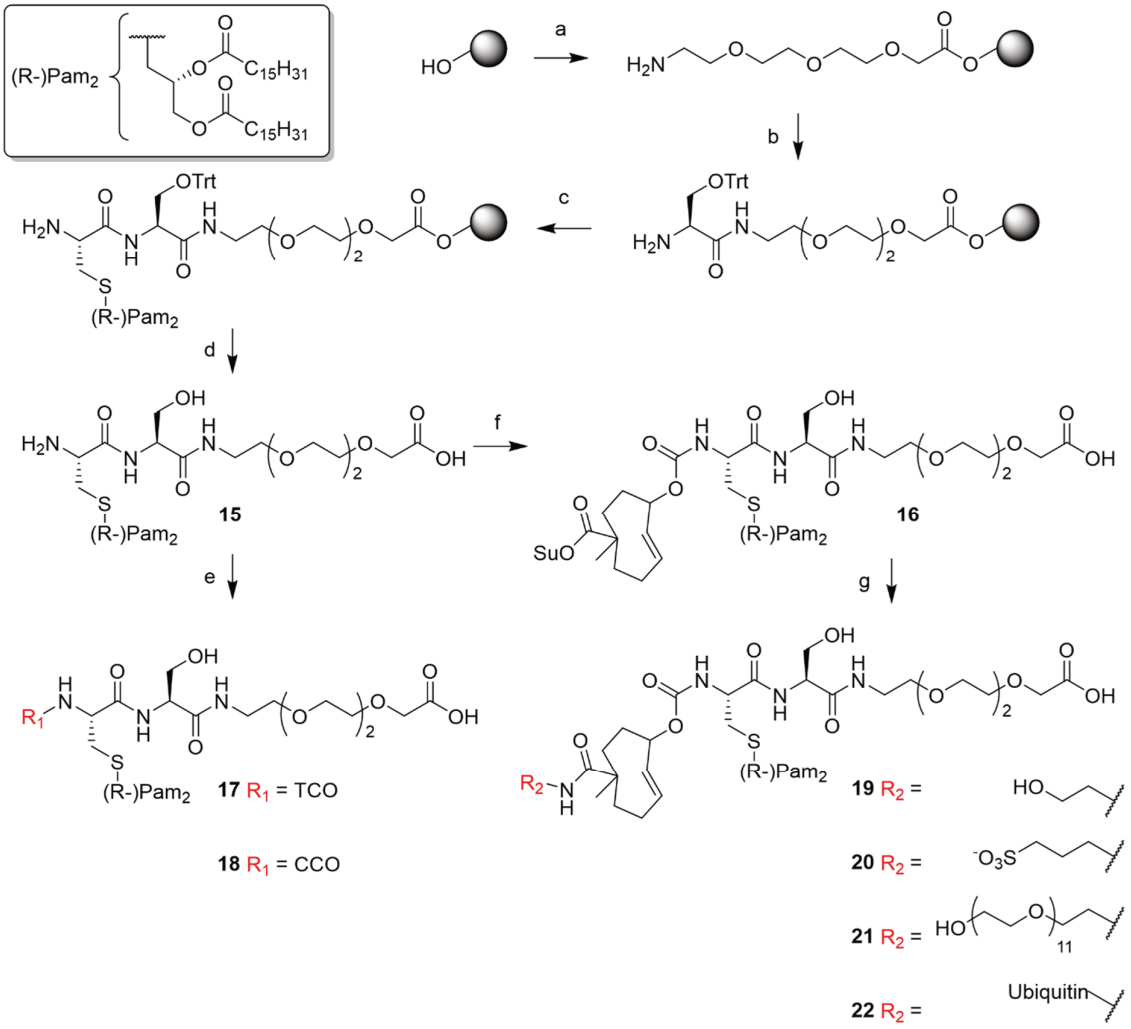

Scheme 4. Synthesis of TCO/CCO-caged P_2CS(TEG) and their hydrophilically extended analogues Reagents and conditions: **a)** (i) Fmoc-NH(TEG)-OH, diisopropylcarbodiimide, DiPEA, DMAP, DCM, r.t., o.n. (ii) benzoic anhydride, DMF, r.t., 30 min (iii) 20% piperidine in DMF, r.t., 10 min (4x); **b)** (i) Fmoc-Ser(Trt)-OH (1 M in DMF), HCTU (1 M in DMF), DiPEA (1 M in DMF), r.t., 4 hrs; (ii) 20% piperidine in DMF, r.t., 10 min (4x); **c)** (i) compound **6** (1 M in DCM), HCTU (1 M in DCM), DiPEA (1 M in DCM), r.t., 4 hrs; (ii) 20% piperidine in DMF, r.t., 10 min (4x); **d)** 20% TFA, 2.5% TIS, 2.5% H_2O in DCM, r.t., 30 min, 29% over 7 steps; **e)** Compound **17**: TCO-OSu, DiPEA, DMSO, r.t., o.n., 18% after RP-HPLC; compound **18**: CCO-OSu, DiPEA, DMSO, r.t., o.n., 20% after RP-HPLC **f)** TCO-$(OSu)_2$, DiPEA, DMF, r.t., o.n.; **g)** Compound **19**: ethanolamine, DMF, r.t., o.n.; compound **20**: homotaurine **13**, DiPEA, DMF, r.t., 7 days; compound **21**: DDEG, DMF, r.t., 40 hrs; compound **22**: ubiquitin, DiPEA, DMSO, r.t., 7 days

First, the ligand P_2CS(TEG) was synthesized on-resin for ease of purification of the intermediates (Scheme **4**). Then, either CCO-NHS, TCO-NHS or TCO-bis-NHS is reacted with the crude N-terminal amine. The intermediate compound **16** is purified by HPLC and consequently conjugated

with ethanolamine, homotaurine, dodecaethylene glycol or ubiquitin. Dodecaethylene glycol was obtained via a modified procedure from a recent publication describing the synthesis of monodisperse PEG derivatives.[27] Interestingly, in all conjugations a minor byproduct was observed which corresponded with a molecular mass reduction of 18 amu, indicating loss of a H_2O molecule. This can be ascribed to the conversion of the serine residue to a dehydroalanine, or by the cyclization with the C-terminal carboxylic acid. It was, however, not investigated further. Also, in the conjugation with homotaurine a major byproduct was observed which again corresponded with the molecular mass of hydrolyzed NHS-ester. Ubiquitin carries seven lysine residues, as well as an N-terminal amine, which can all react with the NHS-ester, so multiple regioisomers as well as a varying ligand-to-protein ratios can be expected. When the reaction mixture was purified with HPLC, ubiquitin carrying one ligand was able to be separated from ubiquitin carrying two or more ligands. Moreover, fractions containing the same molecular mass of mono-conjugated ubiquitin but having a different retention time were isolated, indicating separation of different isoforms of the mono-conjugated ubiquitin.

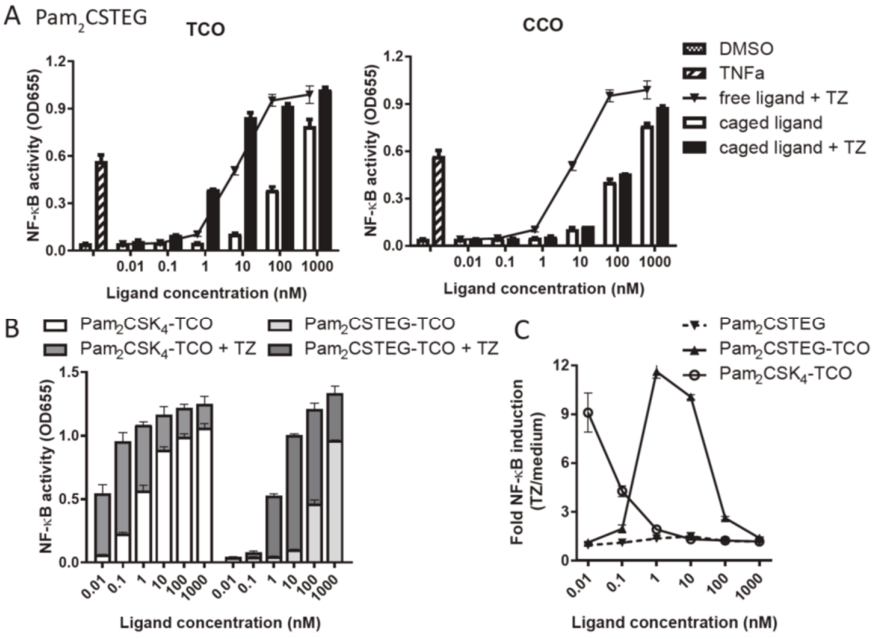

Figure 5. Evaluation of TCO/CCO-caged P_2CS(TEG) in comparison to TCO-caged P_2CSK_4. A/B) THP1-Dual reporter cells were pre-incubated with the indicated ligands for 45min. Fresh medium +/- tetrazine was added and after 24hrs NF-κB activity was measured in the culture supernatant using a SEAP colorimetric assay. C) Fold NF-κB inductions were calculated from the data in (B) by dividing the level of NF-κB activation after decaging (+TZ) over the residual activity in absence of the uncaging reagent. Experiment was carried out by Timo Oosenbrug (LUMC).

First, the effect of substituting the tetralysine linker for the triethylene glycol was assessed by quantifying the NF-κB activity induced by both ligands in THP1-dual reporter cells (Figure 5). P_2CSK_4 was shown to be 100-fold more active than P_2CS(TEG), indicating a beneficial effect of the tetralysine moiety over the TEG elongation. Residual activity in P_2CS(TEG) was still observed, albeit only at higher concentrations. This effect brings about a widening of the concentration range in which a significant fold NF-κB induction exists (Figure 5C).

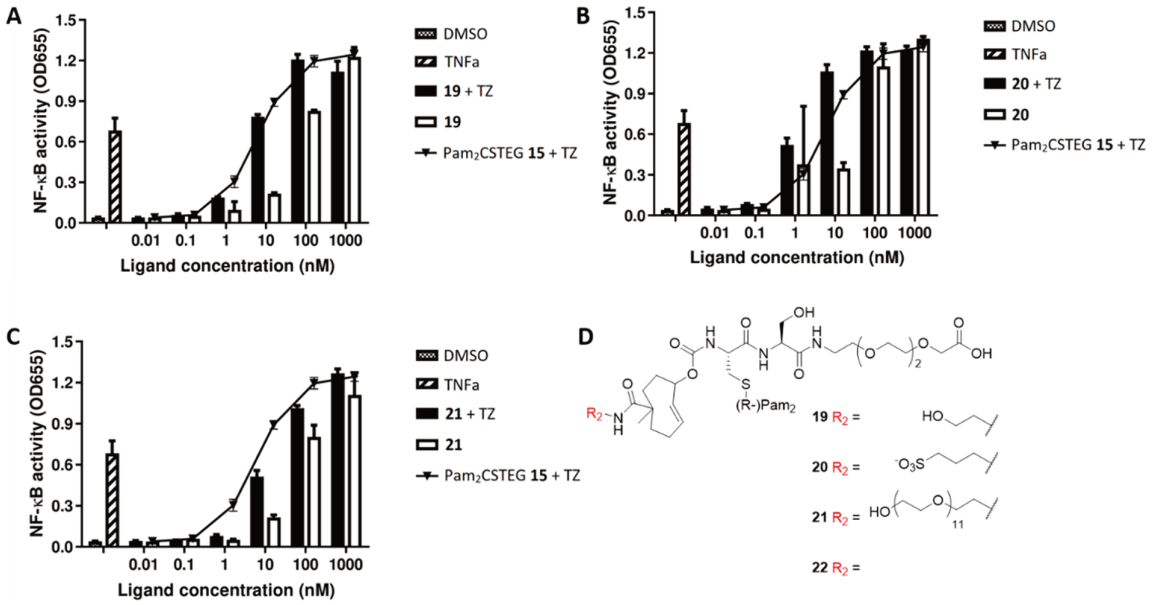

Figure 6. Evaluation of hydrophilically extended TCO-caged P_2CS(TEG) ligands **19-21**. THP1-Dual reporter cells were pre-incubated with the indicated ligands for 45min. Fresh medium +/- tetrazine was added and after 24hrs NF-κB activity was measured in the culture supernatant using a SEAP colorimetric assay. Experiments were carried out by Timo Oosenbrug (LUMC).

Evaluation of the hydrophilically extended caged ligands **19-21**(Figure **6**) revealed that the hydrophobic nature of the cyclooctene is not responsible for the residual activity observed in the caged versions of P_2CSK_4 and P_2CS(TEG), as there was no effect observed for the varying substitutions in comparison to no substitution.

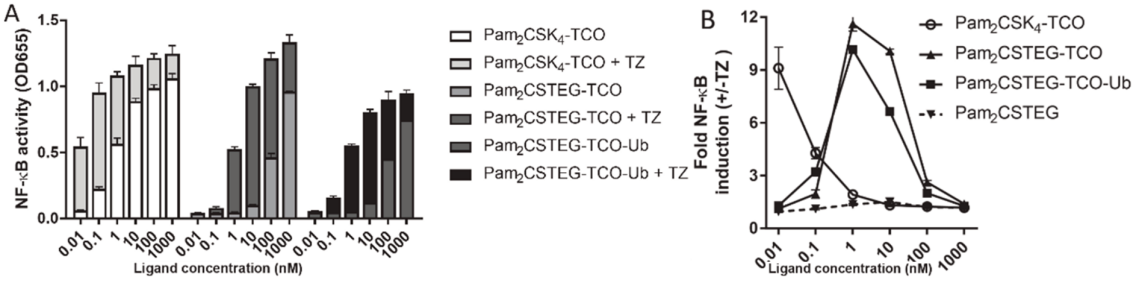

Figure 7. Evaluation of P_2CS(TEG)-TCO-ubiquitin conjugate. A/B) THP1-Dual reporter cells were pre-incubated with the indicated ligands for 45min. Fresh medium +/- tetrazine was added and after 24hrs NF-κB activity was measured in the culture supernatant using an SEAP colorimetric assay. B) Fold NF-kB inductions were calculated from the data in (A) by dividing the level of NF-kB activation after decaging (+TZ) over the residual activity in absence of the uncaging reagent. Experiments were carried out by Timo Oosenbrug (LUMC).

Evaluation of the ubiquitin-conjugated P_2CS(TEG) ligand (Figure **7**) revealed that the potential lack of bulk in the cyclooctene cage is not responsible for the residual activity observed in the parent compounds. This is clearly visualized in Figure **7**B, where the window of activity of TCO-P_2CS(TEG) overlaps neatly with the window of activity of Ubq-TCO-P_2CS(TEG). Perhaps, it is

the metastable nature of the carbamate linkage, prone to hydrolysis, that causes the residual activity observed throughout all experiments. Upon closer inspection of the results outlined in Figure 7A, it seems that the amount of residual activity throughout all ligands tested corresponds closely to the amount of tetrazine-induced activity observed in a 2 log lower concentration. So, >1% prematurely hydrolyzed ligand can already explain the residual activity observed. This hypothesis can be probed by conjugating the cyclooctenes via a more stable linkage towards hydrolysis, for instance the recently published ether-linked TCO cages[28,29]. Ironically, the widened window of activity that was created by substituting the C-terminus, a modification needed to enable substitution on the N-terminus, was already sufficient in continuing investigation of spatiotemporal effects in the TLR2/6 system.

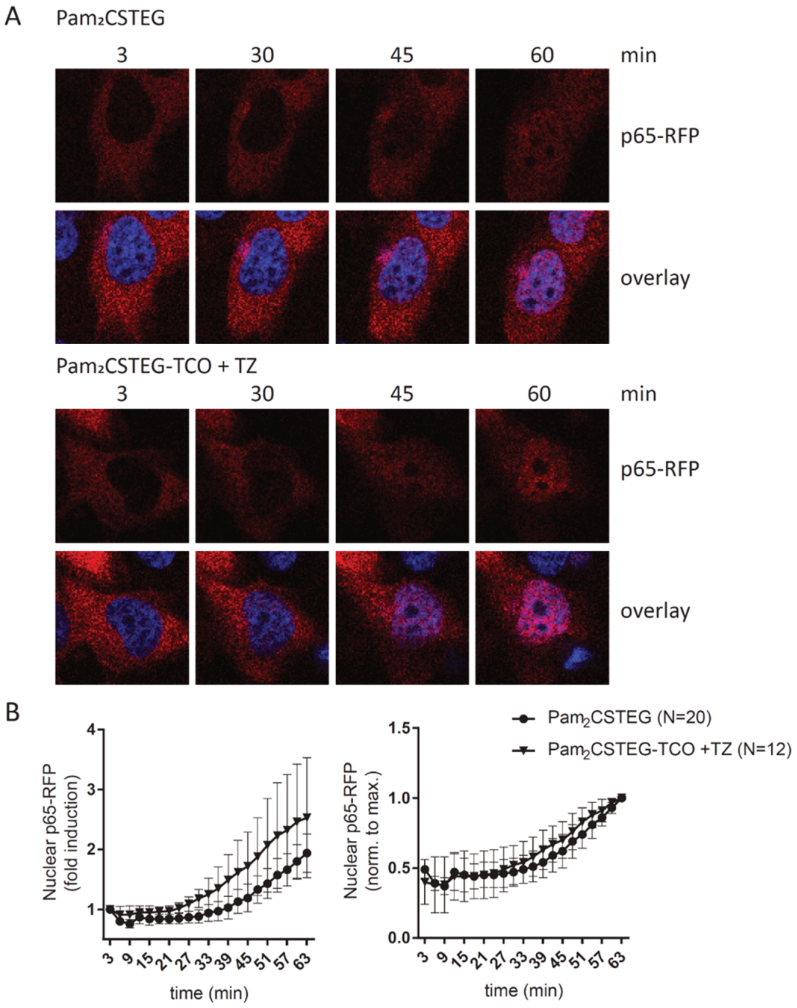

Figure 8. Assessing uncaging speed of TCO-P_2CS(TEG) on live cells. Mel Juso TLR2-YFP p65-RFP cells were pre-incubated for 45 min with 10nM Pam_2CSTEG-TCO. Live cells were imaged after addition of tetrazine (TZ) or after treatment with 10nM free Pam_2CSTEG. A) Representative images of the nuclear translocation of p65-RFP over time. To indicate nuclei, overlays with Hoechst are shown. B) For individual cells the nuclear accumulation of NF-κB was tracked over time. Left: fold increase in nuclear p65-RFP

signal, right: data was normalized per cell to the maximum nuclear p65-RFP signal observed. Experiments were carried out by Timo Oosenbrug (LUMC).

To assess the applicability of the new chemical tool in a temporal-sensitive setting, live cells were primed with TCO-P_2CS(TEG) and treated with tetrazine at t=45min. At this time point, free ligand was added to a separate well and the cells were imaged during the following hour. The Mel Juso cells express p65-RFP, a fluorescently labeled subunit of the NF-kB complex which translocates to the cell nucleus upon TLR2/6 activation. The increase of the RFP-signal in the nucleus was quantified as a function of time (Figure 8B). Gratifyingly, the speed with which the p65-RFP accumulates in the nucleus after treatment with tetrazine coalesces with the p65-RFP nuclear appearance in the cells treated with free ligand at the same time point (Figure 9). Thus, adding tetrazine at a certain time point in the experiment has the same effect as adding free ligand, underlining the benefit of this fast chemo-uncaging in comparison to photo-uncaging, where the cells are usually irradiated for 15 minutes before signal output can be assessed.

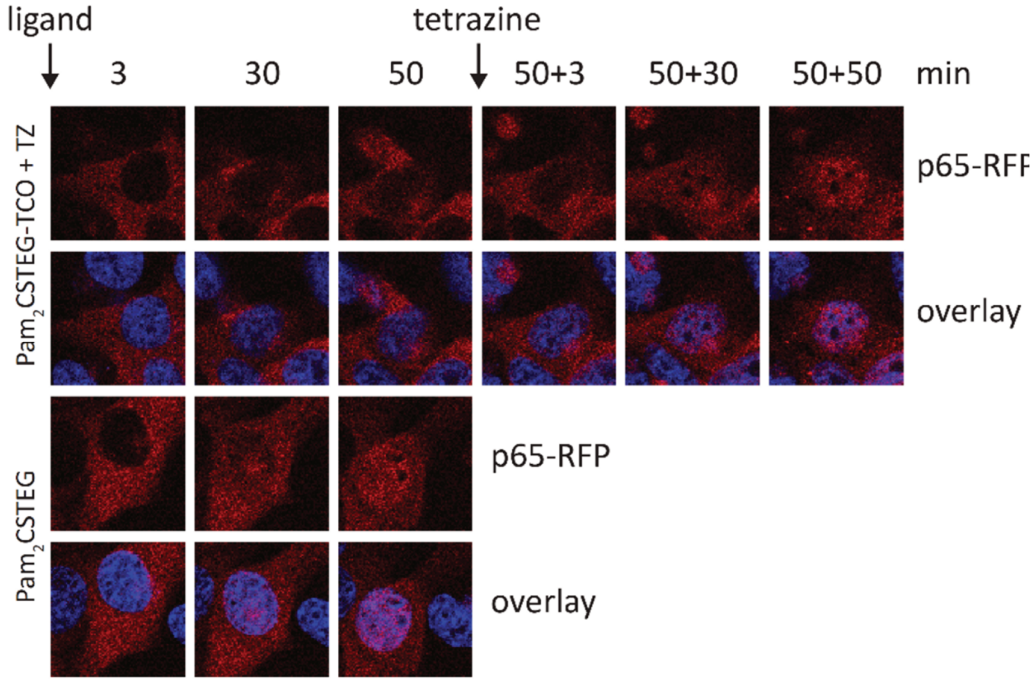

Figure 9. Live human cells respond to TCO-P_2CS(TEG) after tetrazine-mediated uncaging. Live Mel Juso TLR2-YFP p65-RFP cells were imaged over time. Cells were first treated with 10nM caged or free TLR2 ligand. After 50 min the uncaging reagent tetrazine was added and the same cells were imaged for an additional 50 min. To indicate nuclei, overlays with Hoechst are shown. Experiments were carried out by Timo Oosenbrug (LUMC).

It was next investigated whether this approach could be modified to separate two TLR populations: cell surface TLRs and intracellular TLRs. Cell surface-only activation was envisaged through immobilizing a TLR ligand-biotin conjugate on streptavidin-coated wells[2]. However, no tools currently exist to exclusively probe for intracellular activation. For this, either the cell-surface TLR-population has to be selectively inhibited or access to tetrazine reagent has to be limited to only the intracellular TLR-population (Figure 3). Selective inhibition can be achieved by varying the

tetrazine substituents: electron withdrawing moieties have a negligible effect on the ligation, but disfavour the following tautomerisation, thus preventing the elimination. When such a tetrazine is conjugated to a motif limiting cell-permeability, one could selectively silence all the primed cell surface TLRs, while keeping the primed intracellular TLRs intact. Addition of cell-permeable tetrazine would then solely activate intracellular TLR's. Alternatively, the tetrazine can be selectively delivered to endosomes by conjugation to nano-sized beads. Phagocytosis of these beads prior to treatment with chemical tool **17** should lead to accumulation of free ligand inside endosomes containing the nanoparticles only.

Unfortunately, no conjugateable tetrazine is currently described which exerts <1% elimination, so the former strategy cannot be employed without also getting significant cell-surface activation. The latter strategy was therefore selected: amino-modified FluoSpheres (fluorescent 0.2 µm sized polystyrene amine-coated beads, Invitrogen) were decorated with a functional tetrazine (tetrazine **38**, Figure **2**) through an NHS-coupling. The number of amines present on the polystyrene beads is not known, so presence of functional tetrazine was quantified by reacting the beads with a known amount of fluorescently labelled TCO-caged ligand and subjecting the mixture to LC-MS. It was found that 1 µL of a 0.2% bead stock solution can uncage up to 40 pmol of TCO-caged ligand. A strong solvent effect was observed for the uncaging reaction and cellular uptake: when suspended in water, only 7.5 pmol could be uncaged, whereas addition of an equivolumair amount of DMSO increased this to 40 pmol. Also, cellular uptake of the beads appeared to be highly dependent on the presence of DMSO in the suspension. The hydrophobic character of the tetrazine can have a detrimental effect by virtue of aggregation as well as non-specific binding to plastic pipette tips and plastic wells. DMSO can act as a surfactant on the interface of the tetrazines with the aqueous environment, increasing the amount of available and functional tetrazine for uncaging. Alternatively, tetrazines that are functionalized with a water-soluble linker can be used to decorate the nanobeads to combat this effect. The ability of these nanobeads to uncage TCO-bearing TLR ligands *in vitro* is currently awaiting its assessment.

Conclusion

This Chapter describes the use of *trans*-cyclooctene as a suitable cage for preventing TLR2/6 dimerization when conjugated to a TLR2/6 agonist. When present on the N-terminus of the canonical Pam_2CSK_4 TLR2/6 ligand, conditional induction of TLR2 responses could be validated in various murine cell types through application of a tetrazine derivative. Substitution of the C-terminal tetralysine motif to a triethylene glycol linker yielded an TLR2/6 agonist that was more facile to synthesize and allowed for greater derivatization through the enablement of solution-phase chemistry. Simultaneously, this TCO-caged ligand exerts improved performance in human cells; having a lower background activity in a non-tetrazine milieu. Further reducing this background activity through increased disruption of the dimerization interface was probed with this new ligand by appending linkers of various sizes and polarity to the TCO-cage, leading to the finding the unmodified olefin was sufficient in negating most binding interactions at this site of the ligand. Furthermore, it was shown that the kinetics of the uncaging reaction do not induce a detectable

delay in TLR2 activation, allowing for highly precise temporal control over TLR2 activity. Future work will focus on imposing spatial control on this system, through the site-selective delivery of the uncaging reagents.

Acknowledgements

Timo Oosenbrug (LUMC) is acknowledged for the biological evaluation of the compounds described in this Chapter. Mark de Geus is acknowledged for providing *trans*-cyclooctene building blocks, tetrazine derivatives and valuable discussions. RAW Blue macrophages were kindly provided by the laboratory of Professor A. Esser-Kahn (University of Chicago). Dr. Gerbrand J. van der Heden-van Noort (LUMC) is acknowledged for his aid in the purification and characterization of ubiquitin conjugates. Ubiquitin was kindly provided by the laboratory of the late Professor H. Ovaa.

Experimental section

General experimental procedures

General reagents were obtained from Sigma Aldrich, Fluka, and Acros. All reagents were of commercial grade and used as received unless stated otherwise. Solvents used in synthesis were dried and stored over 4Å molecular sieves, except MeOH and ACN which were stored over 3Å molecular sieves. Triethylamine (Et_3N) and Diisopropylethylamine (DiPEA) were stored over KOH pellets. Peptide polymer resins were purchased at Rapp Polymere. Ubiquitin protein was generously provided by the laboratory of the late Dr. H. Ovaa (LUMC, Leiden, The Netherlands). LC-MS analysis was performed on a Finnigan Surveyor HPLC system with a Nucleodur C18 Gravity 3um 50 x 4.60 mm column (detection at 200-600 nm) coupled to a Finnigan LCQ Advantage Max mass spectrometer with ESI or coupled to a Thermo LCQ Fleet Ion mass spectrometer with ESI. The Method used was 10→90% 13.5 min (0→0.5 min: 10% MeCN; 0.5→8.5 min: 10% to 90% MeCN; 8.5→ 11 min: 90% MeCN; 11→13.5 min: 10% MeCN) unless otherwise stated. High resolution mass spectra (HRMS) were recorded on the following machines: Thermo Scientific Q Exactive HF Orbitrap mass spectrometer equipped with an electrospray ion source in positive-ion mode (source voltage 3.5 kV, sheath gas flow 10, capillary temperature 275 °C) with resolution R = 240.000 at m/z 400 (mass range of 150-6000) correlated to an external calibration, or on a Waters Synapt G2-Si (TOF) equipped with an electrospray ion source in positive mode (source voltage 3.5 kV) and LeuEnk (m/z = 556.2771) as internal lock mass. As an exception, compound **22** was measured on the following apparatus: Waters XEVO-G2 XS Q-TOF mass spectrometer equipped with an electrospray ion source in positive mode (source voltage 3.0 kV, desolvation gas flow 900 L/hr, temperature 250 °C) with resolution R = 22000 (mass range m/z = 50-2000) and 200 pg/uL Leu-Enk (m/z = 556.2771) as a "lock mass". HPLC purification was performed on a Gilson HPLC system coupled to a Magerey-Nagel Nucleodur C18 Gravity 5 µm 250 ×10mm column, or on an Agilent 1200 HPLC/6130 MS system coupled to a Magerey-Nagel Nucleodur C18 Gravity 5µm 250×10 mm column or on a Waters autopurifier HPCL/MS system coupled to a Phenomenex Gemini 5µm 150×21.2 mm column.

Compound 1

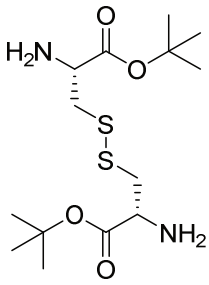

L-Cystine (41.6 mmol, 10.0 g) was dissolved in 70% $HClO_4$ (aq.) (166 mmol, 14.6 mL). *Tert*-butyl acetate (750 mmol, 100 mL) was added and the reaction was stirred at room temperature for 75 hours. TLC-MS indicated complete conversion of the starting material and the reaction mixture was cooled on ice for 30 minutes. 2M NaOH (aq.) (0.17 mol, 6.8 g in 85 mL) was slowly added and the mixture was washed with Et_2O (3x) and EtOAc (3x). The organic layers were combined, dried ($MgSO_4$) and concentrated *in vacuo* to yield the title compound (41 mmol, 14 g, qt.). **^{1}H NMR (400 MHz, $CDCl_3$)** δ = 7.78 (s, 7H), 4.35 (t, *J*=5.9, 2H), 3.38 (m, 4H), 2.04 (d, *J*=2.8, 3H), 1.51 (s, 18H).**^{13}C NMR (101 MHz, $CDCl_3$) δ** = 177.57, 167.66, 85.12, 53.43, 38.62, 27.95.

Compound 2

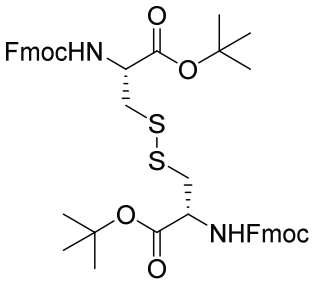

Compound **1** (37 mmol, 13 g) was dissolved in THF (40 mL). Fmoc-OSu (77 mmol, 26 g) and a solution of N-methyl morpholine (112 mmol, 12.3 mL) in THF (20 mL) were added. The mixture was stirred for 2 hours at room temperature when TLC analysis (20% EtOAc in Pnt, R_f=0.6) indicated complete conversion of the starting material. The mixture was poured in EtOAc (500 mL) and washed with 0.5M HCl (aq.) (3x) and brine (1x). The organic layers were combined, dried ($MgSO_4$) and concentrated *in vacuo*. Et_2O (500 mL) was added and the white precipitate was filtered yielding the title compound (18.3 mmol, 14.6 g). The filtrate was concentrated and adsorbed onto Celite. Silica gel column chromatography (10% EtOAc in Pnt → 20% EtOAc in Pnt) yielded the title compound (7.2 mmol, 5.8 g, 68% combined yield). **^{1}H NMR (400 MHz, $CDCl_3$)** δ = 7.79 – 7.69 (m, 4H), 7.57 (d, *J*=7.5, 4H), 7.36 (td, *J*=7.4, 3.0, 4H), 7.27 (t, *J*=7.4, 4H), 5.80 (d, *J*=7.8, 2H), 4.58 (dt, *J*=7.9, 5.3, 2H), 4.35 (dd, *J*=7.3, 2.6, 5H), 4.19 (q, *J*=7.3, 5.6, 2H), 3.20 (qd, *J*=14.1, 5.3, 4H), 1.47 (s, 18H).**^{13}C NMR (101 MHz, $CDCl_3$)** δ = 169.42, 155.80, 143.85, 141.32, 127.75, 127.12, 125.23, 120.02, 83.15, 67.27, 60.46, 54.20, 47.13, 28.05.

Compound 3

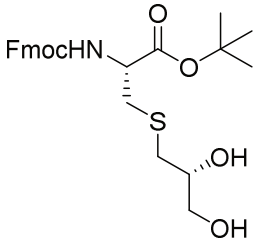

Compound **2** (10 mmol, 8.0 g) was dissolved in THF (100 mL). Zinc powder (7 mmol, 0.46 g, 10 μm) and a solution of MeOH:37% HCl (aq.):98% H_2SO_4 (93:6:1, 50 mL) were added and the reaction was stirred for 15 minutes at room temperature. TLC analysis (20% EtOAc in Pnt, R_f=0.8) indicated complete conversion of the starting material. R-(+)-glycidol (30 mmol, 2.5 mL) was added and the reaction was stirred for 72 hours at room temperature. TLC analysis (80% EtOAc in Pnt, R_f=0.5) indicated complete conversion of the starting material. The mixture was filtered and the filtrate was concentrated *in vacuo*. The concentrate was diluted in DCM and washed with sat. $NaHCO_3$ (aq.) (5x). The aqueous layers were combined and back-extracted with DCM (3x). The organic layers were combined, dried ($MgSO_4$) and concentrated in vacuo. Silica gel column chromatography (60% EtOAc → 70% EtOAc) yielded the title compound (15.5 mmol, 7.35 g, 78%).**^{1}H NMR (400 MHz, $CDCl_3$)** δ = 7.70 (d, *J*=7.5, 2H), 7.63 – 7.50 (m, 2H), 7.35 (t, *J*=7.4, 2H), 7.31 – 7.21 (m, 3H), 6.14 (d, *J*=8.1, 1H), 4.48 (dt, *J*=7.9, 5.6, 1H), 4.35 (d, *J*=7.2, 2H), 4.18 (t, *J*=7.2, 1H), 3.94 (s, 1H), 3.78 (qd, *J*=8.4, 5.5, 4.9, 1H), 3.65 (dd, *J*=11.0, 3.4, 1H), 3.51 (dd, *J*=11.5, 6.3, 1H), 2.96 (qd, *J*=13.9, 5.6, 2H), 2.81 – 2.49 (m, 2H), 1.45 (s, 9H). **^{13}C NMR (101 MHz, $CDCl_3$)** δ = 169.82, 156.05, 143.69, 143.61, 141.12, 127.61, 126.98, 125.04, 119.87, 82.82, 71.01, 67.07, 65.08, 54.46, 46.92, 36.17, 35.28, 27.85.

Compound 4

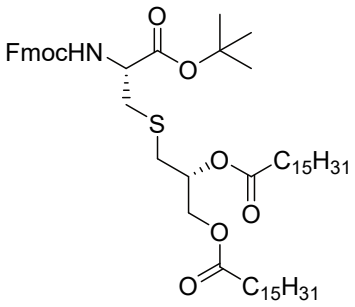

Compound **3** (15.3 mmol, 7.25 g) was dissolved in anhydrous THF (150 mL). Palmitic acid (61 mmol, 16 g), diisopropylcarbodiimide (69 mmol, 11 mL) and DMAP (6.1 mmol, 0.74 g) were added and the reaction was stirred for 2 hours at room temperature. TLC analysis (20% EtOAc in Pnt, R_f=0.5) indicated complete conversion of the starting material. Acetic acid (7 mL) was added and the mixture was concentrated *in vacuo*. The concentrate was dissolved in a minimal amount of warm DCM, after which the solution was carefully diluted with MeOH (>10x V_{DCM}). The mixture was left overnight at room temperature after which the formed crystals were collected by filtration. The mother liquor was concentrated *in vacuo* and subjected to a second crystallization round. The crystals were combined and washed with cold MeOH, yielding the title compound (14.5 mmol, 13.8 g, 95%).**^{1}H NMR (400 MHz, $CDCl_3$)** δ = 7.76 (d, *J*=7.5, 2H), 7.62 (d, *J*=7.5, 2H), 7.40 (t, *J*=7.4, 2H), 7.31 (t, *J*=7.4, 2H), 5.70 (d, *J*=7.7, 1H), 5.16 (qd, *J*=6.3, 3.5, 1H), 4.51 (dt, *J*=7.8, 5.0, 1H), 4.46 – 4.29 (m, 3H), 4.24 (t, *J*=7.2, 1H), 4.16 (dd, *J*=11.9, 5.9, 1H), 3.05 (qd, *J*=13.7, 5.0, 2H), 2.77 (d, *J*=6.4, 2H), 2.30 (q, *J*=7.3, 5H), 1.60 (dqd, *J*=11.6, 8.1, 7.2, 4.7, 6H), 1.49 (s, 10H), 1.36 – 1.16 (m, 60H), 0.88 (t, *J*=6.8, 6H).**^{13}C NMR (101 MHz, $CDCl_3$)** δ = 173.48, 173.19, 169.62, 155.86, 143.96, 141.43, 127.86, 127.22, 125.28, 120.13, 83.15, 70.37, 67.36, 63.60, 54.48, 47.26, 35.51, 34.41, 34.22, 33.43, 32.07, 29.85, 29.81, 29.78, 29.64, 29.51, 29.44, 29.27, 28.12, 25.04, 25.01, 22.84, 14.27.

Compound 5

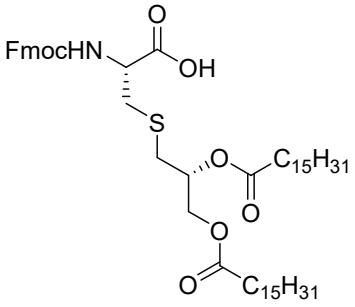

Compound **4** (0.95 mmol, 0.90 g) was dissolved in neat TFA (5 mL) and the mixture was stirred for 1 hour at room temperature. TLC analysis (20% EtOAc in Pnt, R_f=0.2) indicated complete conversion of the starting material. The mixture was concentrated *in vacuo* and co-evaporated with toluene (3x) yielding the title compound (0.95 mmol, 0.85 g).**^{1}H NMR (400 MHz, $CDCl_3$)** δ = 9.69 (s, 1H), 7.74 (d, *J*=7.5, 2H), 7.60 (d, *J*=7.5, 2H), 7.38 (t, *J*=7.5, 2H), 7.29 (t, *J*=7.4, 2H), 5.92 (d, *J*=7.9, 1H), 5.25 – 5.03 (m, 1H), 4.75 – 4.48 (m, 1H), 4.38 (ddt, *J*=16.2, 12.0, 7.0, 3H), 4.22 (t, *J*=7.0, 1H), 4.15 (dd, *J*=12.0, 6.2, 1H), 3.29 – 2.94 (m, 2H), 2.90 – 2.53 (m, 2H), 2.30 (q, *J*=7.7, 4H), 1.58 (td, *J*=7.4, 4.0, 4H), 1.25 (q, *J*=7.8, 5.1, 52H), 0.88 (t, *J*=6.6, 6H).**^{13}C NMR (101 MHz, $CDCl_3$)** δ = 173.86, 156.34, 143.72, 141.37, 127.85, 127.20, 125.24, 120.08, 70.39, 67.64, 63.72, 47.11, 34.67, 34.40, 34.19, 32.99, 32.04, 29.83, 29.79, 29.76, 29.63, 29.49, 29.41, 29.24, 29.21, 25.00, 24.96, 22.81, 14.24.

Resin-bound peptide 6.1

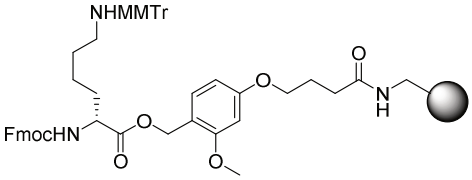

Tentagel S AC resin (0.5 g, 125 µmol) was swollen in DMF and treated with Fmoc-Lys(MMTr)-OH (375 µmol, 241 mg), DIC (375 µmol, 58 µL) and DMAP (cat. amount). The syringe was shaken overnight and consequently washed with DMF (5x), DCM (5x) and Et_2O (3x). Dry weight loading analysis indicated a complete conversion (592 mg, 138 µmol).

Resin-bound peptide 6.2

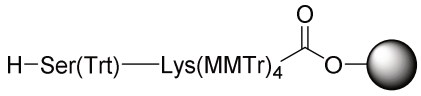

The following SPPS cycle was carried out four times to form the serine-tetralysine pentapeptide: Resin bound lysine **6.1** was swollen in DMF and treated with a solution of 20% piperidine in DMF for 10 min. (4x) and consequently washed with DMF (5x). The resulting resin was treated with HCTU (1 mL, 0.6 M in DMF), amino acid (1 mL, 0.6 M in DMF) and lastly DiPEA (1 mL, 0.6 M in DMF). The syringe was shaken for 2 hours and consequently washed with DMF (5x). A solution of 5% acetic anhydride in 0.1 M DiPEA in DMF was added and the syringe was shaken for 10 min. The resin was washed with DMF (5x), treated with a solution of 20% piperidine in DMF for 10 min. (4x) and consequently washed with DMF (5x).

Resin-bound peptide 6.3

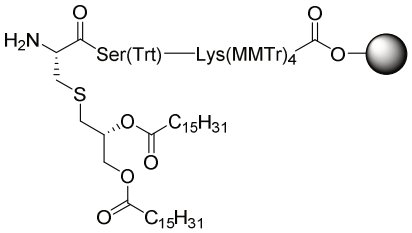

Resin-bound pentapeptide **6.2** was swollen in DMF and treated with HCTU (1 mL, 0.6 M in DMF), Fmoc-*R*-Pam_2Cys-OH (1 mL, 0.6 M in DMF) and lastly DiPEA (1 mL, 0.6 M in DMF). The syringe was shaken for 2 hours and consequently washed with DMF (5x). A solution of 5% acetic anhydride in 0.1 M DiPEA in DMF was added and the syringe was shaken for 10 min. The resin was washed with DMF (5x), treated with a solution of 20% piperidine in DMF for 10 min. (4x) and consequently washed with DMF (5x), DCM (3x) and dried with Et_2O (3x) for prolonged storage.

Resin-bound peptide 6.4

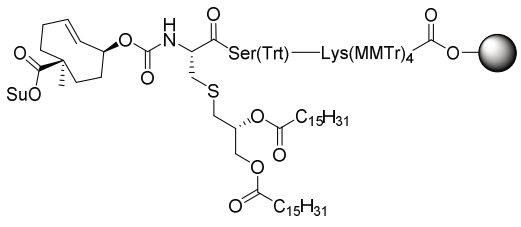

Resin-bound hexapeptide **3** (198 mg, 30 µmol) was swollen in DMF and DiPEA (60 µmol, 11 µL) and bis functionalized TCO-OSu_2 (60 µmol, 25 mg) were added and the reaction syringe was shaken overnight. LC-MS analysis of a small amount of TFA-treated resin indicated complete conversion of the starting material. The resin was washed with DMF (3x) and DCM (3x).

Compound 7

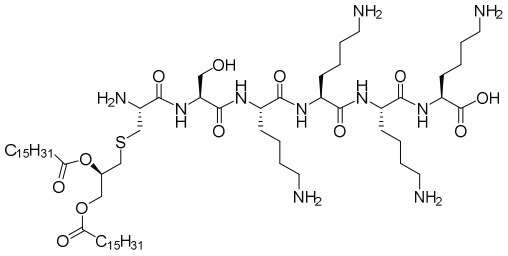

Resin-bound hexapeptide **6.3** (10 µmol, 45 mg) was swollen in DCM and consequently treated with a solution of 20% TFA, 2.5% TIS and 2.5% H_2O in DCM. The syringe was shaken for 1 hour and emptied in a tube containing a 1:1 mixture of Pnt:Et_2O at -20°C. The resulting precipitation was collected by centrifugation and removal of the supernatant. The crude pellet was purified by reverse-phase HPLC (Gradient: 50% AcN + 90% (H_2O+0.1% TFA) to 90% AcN + 10% (H_2O+0.1% TFA)) to obtain compound **6** (0.65 µmol, 0.83 mg, 6.5%). **HRMS**: $[M+H]^+$ calculated for $C_{65}H_{127}N_{10}O_{12}S$ 1271.93502; found 1271.93487

Compound 8

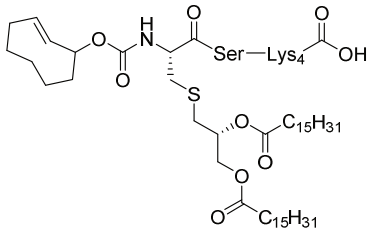

Resin-bound hexapeptide **3** (63 mg, 16 µmol) was swollen in DMF and DiPEA (20 µmol, 3.5 µL) and TCO-OSu (20 µmol, 5.1 mg) were added and the reaction syringe was shaken overnight. LC-MS analysis of a small amount of TFA-treated resin indicated complete conversion of the starting material. The resin was washed with DMF (3x) and DCM (3x). A solution of 5% TFA, 2.5% TIS, 2.5% H_2O in DCM was added and the reaction vessel was shaken for 15 min. The syringe was emptied in a 0°C solution of 50% Pnt in Et_2O (total volume = 40 mL) and put in a -20°C freezer overnight. The tube was then centrifuged for 90min at 4°C after which a pellet was visible. The tube was decanted and the pellet was purified on HPLC (TFA) to yield compound the title compound (1.2 µmol, 1.7 mg, 7.5%). **LC-MS (5090, C18, H_2O/AcN + TFA):** 1424.02 (z=1, simulated), 1423.87 (z=1, observed), 1536.80 (z=1, TFA adduct), 1650.07 (z=1, 2*TFA adduct) **HRMS**: $[M+H]^+$ calculated for $C_{74}H_{138}N_{10}O_{14}S$ 1424.01875; found 1424.01805

Compound 9

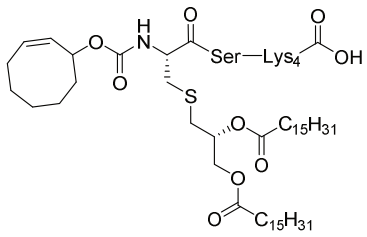

Resin-bound hexapeptide **6.3** (45 mg, 11 µmol) was swollen in DMF and DiPEA (11 µmol, 2 µL) and CCO-OSu (20 µmol, 5.1 mg) were added and the reaction syringe was shaken overnight. LC-MS analysis of a small amount of TFA-treated resin indicated complete conversion of the starting material. The resin was washed with DMF (3x) and DCM (3x). A solution of 5% TFA, 2.5% TIS, 2.5% H_2O in DCM was added and the reaction vessel was shaken for 15 min. The syringe was emptied in a 0°C solution of 50% Pnt in Et_2O (total volume = 40 mL) and put in a -20°C freezer overnight. The tube was then centrifuged for 90min at 4°C after which a pellet was visible. The tube was decanted and the pellet was purified on HPLC (TFA) to yield compound the title compound (0.31 µmol, 0.44 mg, 2.8%). **LC-MS (5090, C18, H_2O/AcN + TFA):** 1424.02 (z=1, simulated), 1423.87 (z=1, observed), 1536.67 (z=1, TFA adduct), 1650.27 (z=1, 2*TFA adduct) **HRMS**: $[M+H]^+$ calculated for $C_{74}H_{139}N_{10}O_{14}S$ 1424.01875; found 1424.01805

Compound 10

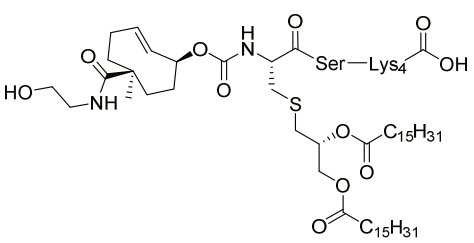

Resin-bound hexapeptide **6.4** (15 µmol, 100 mg) was swollen in DCM and ethanolamine (75 µmol, 4.5 µL) was added. The syringe was shaken overnight after which LC-MS analysis of a small amount of TFA-treated resin indicated complete conversion of the starting material. The resin was washed with DCM (3x). A solution of 5% TFA, 2.5% TIS, 2.5% H_2O in DCM was added and the reaction vessel was shaken for 30 minutes (repeated 1x). The combined flowthroughs were diluted with toluene and carefully evaporated and co-evaporated with toluene (2x). **LC-MS (5090, C18, H_2O/AcN + TFA):** 1525.06 (z=1, simulated), 1524.87 (z=1, observed), 1638.80 (z=1, TFA adduct), 1751.67 (z=1, 2*TFA adduct)

Compounds 11 and 12

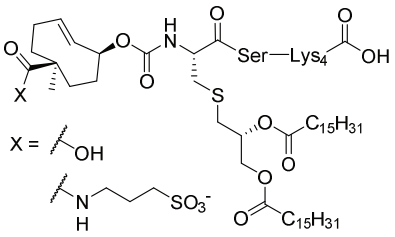

Resin-bound hexapeptide **6.4** (20 µmol, 140 mg) was swollen in DMSO and homotaurine (100 µmol, 14 mg) and DiPEA (100 µmol, 17 µL) were added. The syringe was shaken overnight after which LC-MS analysis of a small amount of TFA-treated resin indicated complete conversion of the starting material to the product and hydrolyzed NHS-ester. The resin was washed with DCM (3x). A solution of 5% TFA, 2.5% TIS, 2.5% H_2O in DCM was added and the reaction vessel was shaken for 30 minutes (repeated 1x). The combined flowthroughs were diluted with toluene and carefully evaporated and co-evaporated with toluene (2x). **LC-MS (Homotaurine product, 5090, C18, H_2O/AcN + TFA):** 1602.06 (z=1, simulated), 1602.73 (z=1, observed), 1715.80 (z=1, TFA adduct), 1829.40 (z=1, 2*TFA adduct). **LC-MS (Carboxylic acid product, 5090, C18, H_2O/AcN + TFA):** 1481.04 (z=1, simulated), 1480.93 (z=1, observed), 1593.73 (z=1, TFA adduct), 1707.53 (z=1, 2*TFA adduct)

Compound 13

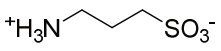

1,3-propanesultone (10 mmol, 1.2 g) was dissolved in 7N methanolic ammonia at 0°C under a nitrogen atmosphere. The mixture was heated to room temperature and stirred for 2 hours. TLC analysis (AcN, R_f(1,3-propanesultone) = 0.9) indicated complete conversion of the starting material. The reaction mixture was poured in Et_2O (200 mL) and centrifuged in 50 mL tubes. The tubes were decanted and the pellet was collected and dried *in vacuo*, yielding the title compound (8.4 mmol, 1.2 g, 84%).**^{1}H NMR (400 MHz, DMSO-*d*$_6$)** δ = 7.62 (s, 3H), 2.92 (t, *J*=7.0, 2H), 2.58 (t, *J*=6.8, 2H), 1.87 (p, *J*=6.9, 2H).**^{13}C NMR (101 MHz, DMSO)** δ = 48.74, 38.69, 23.30.

Resin-bound compound 14.1

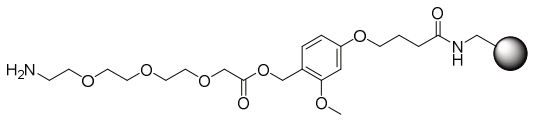

Tentagel S AC resin (0.5 mmol, 2.0 g) was swollen in dry DCM and treated with diethylene glycol 2-aminoethyl acetic acid (2.5 mmol, 518 mg), DIC (2.5 mmol, 389 µL) and DMAP (cat. amount). The reaction syringe was shaken overnight after which the resin was washed with DCM (5x). The resin was treated with a solution of pyridine (2.5 mmol, 201 µL) in DMF after which a solution of benzoic anhydride (2.5 mmol, 556 mg) in DMF was added and the reaction syringe was shaken for 30 min. The resin was washed with DMF (5x) after which the resin was treated with a solution of 20% piperidine in DMF for 10 min. (4x) and consequently washed with DMF (5x) and DCM (3x).

Resin-bound compound 14.2

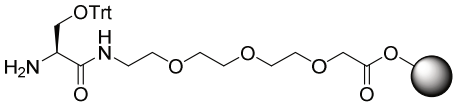

Resin-bound triethylene glycolamine **14.1** (0.5 mmol) was swollen in DMF. Fmoc-Ser(Trt)-OH (1 mmol, 570 mg), HCTU (1 mmol, 414 mg) and DiPEA (1 mmol, 174 µL) were added as 1 M solutions in DMF. The reaction syringe was shaken for 4 hours after which the resin was washed with DMF (3x) and DCM (3x). The resin was treated with a solution of 20% piperidine in DMF for 10 min. (4x) and consequently washed with DMF (5x) and DCM (3x).

Resin-bound compound 14.3

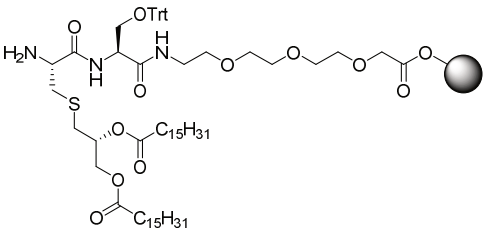

Resin-bound compound **14.2** (0.4 mmol, 1.74 g) was swollen in DCM. Compound **5** (0.5 mmol, 447 mg), HCTU (0.5 mmol, 207 mg) and lastly DiPEA (0.5 mmol, 87 µL) were added as 1 M solutions in DCM. The reaction syringe was shaken for 4 hours after which the resin was washed with DCM (5x). LC-MS analysis of a small amount of TFA-treated resin indicated complete conversion of the starting compound. The resin was swollen in DMF and treated with a solution of 20% piperidine in DMF for 10 min. (4x) and consequently washed with DMF (5x) and DCM (3x).

Compound 15

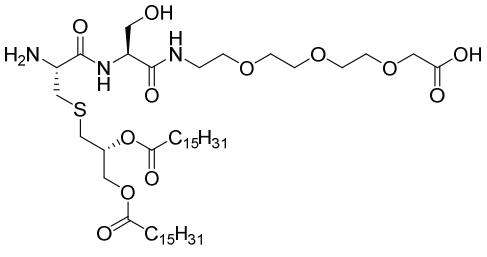

Resin-bound compound **14.3** (0.4 mmol, 2.06 g) was swollen in DCM. A mixture of 20% TFA, 2.5% TIS and 2.5% H_2O in DCM was added and the syringe was shaken for 30 min. The syringe was emptied in a flask containing 50 mL of toluene and the mixture was concentrated *in vacuo*. After co-evaporation with toluene (3x), the crude was purified on HPLC (TFA) to obtain compound **15** (116 µmol, 110 mg, 29%). **LC-MS (7090, C18, H_2O/AcN + TFA):**

948.66 (z=1, simulated), 948.47 (z=1, observed), 970.53 (z=1, Na adduct), 992.47 (z=1, 2*Na adduct) **HRMS**: $[M+H]^+$ calculated for $C_{49}H_{94}N_3O_{12}S$ 948.65527; found 948.65492

Compound 16

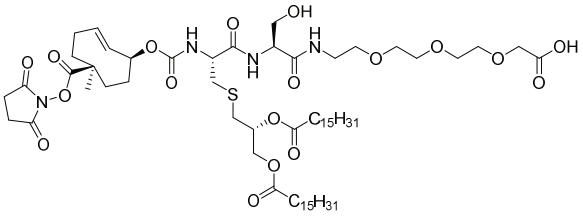

Compound **15** (10 µmol, 9.5 mg) was dissolved in dry DMF (200 µL) in an eppendorf tube (1.5 mL). Dual-functionalized TCO-OSu (20 µmol, 8.4 mg) and DiPEA (20 µmol, 3.5 µL) were added. The tube was shaken for 20 hours after which LC-MS indicated depletion of the starting material. The crude reaction mixture was used as is for consequent reactions. **LC-MS (5090, DiPhenyl, H_2O/AcN + TFA):** 1256.74 (z=1, simulated), 1255.50 (z=1, observed), 1277.67 (z=1, Na adduct), 1300.33 (z=1, 2*Na adduct)

Compound 17

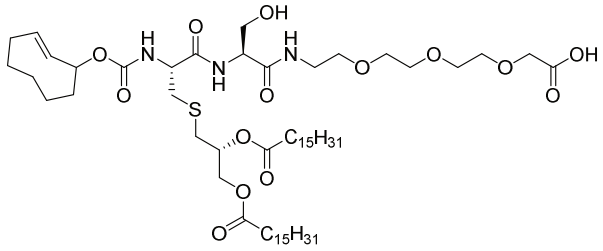

Compound **15** (10 µmol, 9.5 mg) was dissolved in dry DMSO (200 µL) in an eppendorf tube (1.5 mL). TCO-OSu (20 µmol, 5.4 mg) and DiPEA (20 µmol, 3.5 µL) were added. The tube was shaken overnight after which LC-MS (5090, diphenyl column, TFA) indicated complete conversion of the starting material. The crude mixture was directly injected in the HPLC to obtain compound **17** (1.8 µmol, 2.0 mg, 18%). **LC-MS (5090, DiPhenyl, H_2O/AcN + TFA):** 1101.72 (z=1, simulated), 1100.42 (z=1, observed), 1122.67 (z=1, Na adduct), 1145.17 (z=1, 2*Na adduct). **HRMS**: $[M+H]^+$ calculated for $C_{58}H_{106}N_3O_{14}S$ 1100.73900; found 1100.73821

Compound 18

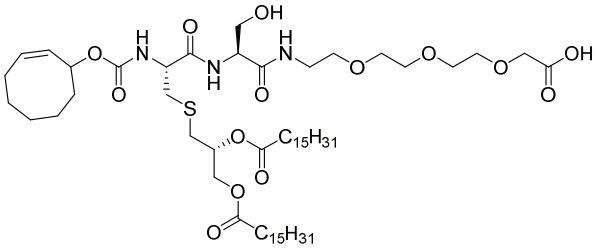

Compound **15** (10 µmol, 9.5 mg) was dissolved in dry DMSO (200 µL) in an eppendorf tube (1.5 mL). CCO-OSu (20 µmol, 5.4 mg) and DiPEA (20 µmol, 3.5 µL) were added. The tube was shaken overnight after which LC-MS (5090, diphenyl column, TFA) indicated complete conversion of the starting material. The crude mixture was directly injected in the HPLC to obtain compound **18** (2.0 µmol, 2.2 mg, 20%).**LC-MS (5090, DiPhenyl, H_2O/AcN + TFA):** 1101.72 (z=1, simulated), 1100.25 (z=1, observed), 1122.58 (z=1, Na adduct), 1144.50 (z=1, 2*Na adduct). **HRMS**: $[M+H]^+$ calculated for $C_{58}H_{106}N_3O_{14}S$ 1100.73900; found 1100.73819

Compound 19

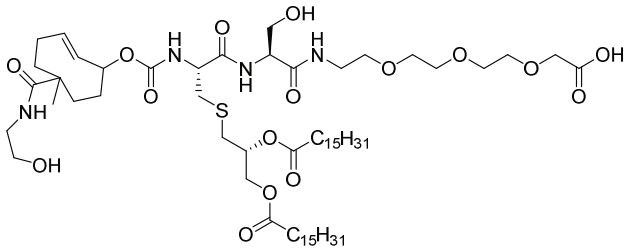

Compound **16** (max. 8.4 µmol in DMF) was put in an eppendorf tube (1.5 mL). Ethanolamine (200 µmol, 12 µL) was added and the tube was shaken overnight at room temperature. LC-MS indicated complete conversion of the starting material. Water (1 mL) was added and the mixture was lyophilized to extrude DMF. The crude was dissolved in DMSO and purified by HPLC (diphenyl, TFA) to obtain the title compound (1.29 mg, 1.1 µmol, 13%). **LC-MS (5090, DiPhenyl, H_2O/AcN + TFA):** 1201.79 (z=1, simulated), 1201.68 (z=1, observed). **HRMS**: $[M+H]^+$ calculated for $C_{62}H_{113}N_4O_{16}S$ 1201.78668; found 1201.78587

Compound 20

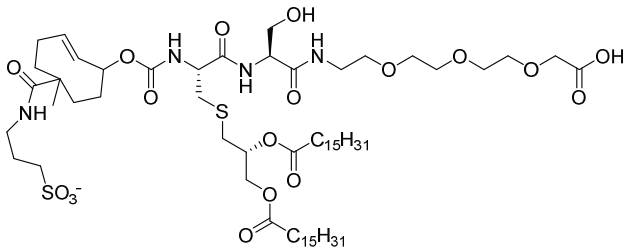

Compound **16** (5 µmol in DMF) was put in an eppendorf tube (1.5 mL). Homotaurine **13** (15 µmol, 2.1 mg) and DiPEA (15 µmol, 2.6 µL) were added and the tube was shaken for 7 days. LC-MS indicated complete conversion of the starting material. Water (1 mL) was added and the mixture was lyophilized to extrude DMF. The crude was dissolved in DMSO and purified by HPLC (diphenyl, TFA) to obtain the title compound (0.86 µmol, 1.1 mg, 17%).**LC-MS (5090, DiPhenyl, H_2O/AcN + TFA):** 1279.76 (z=1, simulated), 1279.42 (z=1, observed) **HRMS**: $[M+H]^+$ calculated for $C_{63}H_{115}N_4O_{18}S_2$ 1279.76423; found 1279.76366

Compound 21

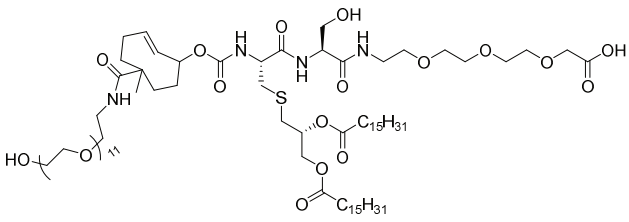

Compound **16** (max. 10 µmol in 200 µL DMF) was put in an eppendorf tube (1.5 mL). Compound **28** (50 µmol, 27 mg) was added and the tube was shaken for 40 hours. LC-MS (5090, diphenyl, TFA) indicated complete conversion of the starting material. Water (1 mL) was added and the mixture was lyophilized to extrude DMF. The crude was dissolved in DMSO and purified by HPLC (diphenyl, TFA) to obtain compound **21** (1.7 µmol, 2.9 mg, 17%). **LC-MS (5090, DiPhenyl, H_2O/AcN + TFA):** 1685.08 (z=1, simulated), 1685.17 (z=1, observed), 1707.83 (z=1, Na adduct), 843.83 (z=2, M+2H). **HRMS**: $[M+H]^+$ calculated for $C_{84}H_{157}N_4O_{27}S$ 1686.07504; found 1686.07431

Compound 22

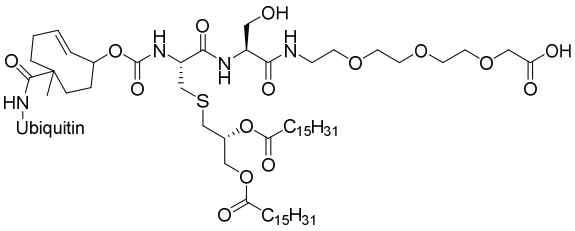

Ubiquitin (0.53 µmol, 4.8 mg, endotoxin-free, Worthington) was dissolved in dry DMSO (160 µL) in an eppendorf tube (1.5 mL). DiPEA (6 µmol, 1 µL) in dry DMSO (20 µL) and compound **16** (0.53 µmol in stock solution) were added. The tube was shaken for 7 days after which HRMS showed formation of single and dual conjugated ubiquitin constructs. The crude was purified on HPLC (1090, C18, TFA) to obtain two separate fractions (A and B) containing products with the mass corresponding to mono-functionalized ubiquitin (Fraction A: 0.65 mg, 67 nmol, 13%; Fraction B: 0.42 mg, 43 nmol, 8.1%). **HRMS:** $[M+10H]^{10+}$ calculated for $C_{438}H_{734}N_{108}O_{133}S_2$ 971.5438; found 971.5424;

Compound 23

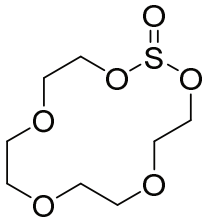

Tetraethylene glycol (5.2 mmol, 1.0 g), DiPEA (25 mmol, 4.4 mL) and DMAP (0.26 mmol, 31 mg) were dissolved in DCM (100 mL) and cooled to 0°C. $SOCl_2$ (10 mmol, 0.75 mL) was dissolved in DCM, cooled to 0°C and added to the reaction mixture over a period of 1 hour. After addition was complete, the mixture was stirred for another hour at 0°C after which brine was added to the mixture. The water layer was washed with DCM (3x). The organic layers were combined, dried ($MgSO_4$) and concentrated *in vacuo*. The crude was used *as is* in the following reaction.

Compound 24

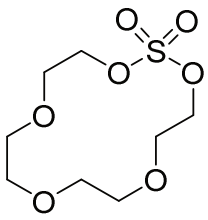

Compound **23** (5.2 mmol, 1.2 g) was dissolved in a mixture of acetonitrile (40 mL), DCM (40 mL) and H_2O (60 mL) and cooled to 0°C. $NaIO_4$ (5.2 mmol, 1.1 g) and $RuCl_3.3H_2O$ (0.077 mmol, 20 mg) were added and the mixture stirred for 1 hour at to room temperature. The mixture was transferred to a separatory funnel and the DCM layer was collected. The water layer was washed with DCM (3x). The organic layers were combined, dried ($MgSO_4$), filtered over Celite and concentrated *in vacuo*. Silica gel column chromatography (50% EtOAc in Pnt, R_f=0.3) yielded the title compound (4.7 mmol, 1.2 g, 91% over 2 steps). **^{1}H NMR (400 MHz, $CDCl_3$)** δ = 4.53 – 4.43 (m, 4H), 3.84 (dd, *J*=5.5, 4.6, 4H), 3.74 – 3.59 (m, 8H). **^{13}C NMR (101 MHz, $CDCl_3$)** δ = 72.14, 70.48, 70.39, 68.23.

Compound 25

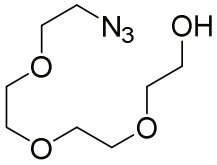

Compound **24** (1.0 mmol, 0.26 g) was dissolved in DMF (5 mL). NaN_3 (1.5 mmol, 0.098 g) was added and the mixture was stirred for 1 hour at 60°C. TLC analysis (50% EtOAc in Pnt, R_f(starting material)=0.3) indicated complete conversion of the starting material. The DMF was evaporated *in vacuo* and the concentrate was diluted with THF (5 mL). H_2O (3 mmol, 54

µL) and 98% H_2SO_4 (1.5 mmol, 80 µL) were added and the mixture was stirred for 1 hour at reflux temperature. TLC analysis (100% EtOAc, R_f=0.4) indicated complete conversion of the starting material. The mixture was poured into H_2O and washed with DCM (3x). The organic layers were combined, dried ($MgSO_4$) and concentrated *in vacuo* to yield the title compound (1.0 mmol, 219 mg, qt.). **^{1}H NMR (400 MHz, $CDCl_3$)** δ = 3.75 – 3.70 (m, 2H), 3.68 (d, *J*=2.5, 11H), 3.63 – 3.58 (m, 2H), 3.40 (dd, *J*=5.6, 4.5, 2H), 3.18 (s, 1H).**^{13}C NMR (101 MHz, $CDCl_3$)** δ = 72.38, 70.45, 70.40, 70.34, 70.10, 69.81, 61.37, 50.43.

Compound 26

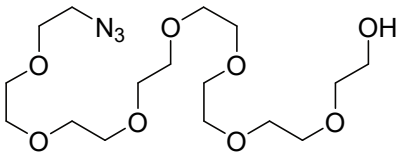

NaH (1.0 mmol, 0.040 g) was suspended in anhydrous THF (10 mL) and cooled to 0°C under a nitrogen atmosphere. To this mixture was added a solution of compound **25** (1.0 mmol, 0.22 g) in anhydrous THF (2.5 mL) and stirred for 15 minutes at 0°C. A solution of compound **24** (0.83 mmol, 0.21 g) in THF (1.7 mL) was added to the reaction mixture and stirred for 2 hours at 0°C. Then the mixture was heated to 50°C for 20 minutes after which TLC analysis (100% EtOAc, R_f=0.1) indicated complete conversion of the starting material. H_2O (3 mmol, 54 µL) and 98% H_2SO_4 (1.5 mmol, 80 µL) were added and the mixture was stirred for 1 hour at reflux temperature. The mixture was poured in H_2O and washed with DCM (3x). The organic layers were combined, dried ($MgSO_4$) and concentrated *in vacuo*. Silica gel column chromatography (DCM→0.75% MeOH in DCM, Δ=0.25%) yielded the title compound (0.47 mmol, 0.19 g, 56%). **^{1}H NMR (400 MHz, $CDCl_3$)** δ = 3.75 – 3.71 (m, 2H), 3.71 – 3.63 (m, 26H), 3.63 – 3.58 (m, 2H), 3.39 (t, *J*=5.1, 2H), 2.92 (s, 1H). **^{13}C NMR (101 MHz, $CDCl_3$)** δ = 72.51, 70.64, 70.61, 70.58, 70.56, 70.51, 70.49, 70.28, 69.99, 61.62, 50.62.

Compound 27

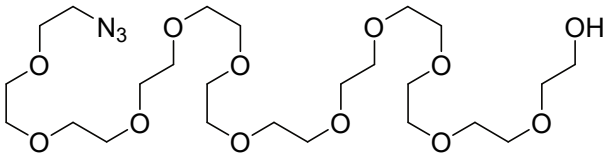

NaH (0.5 mmol, 0.020 g) was suspended in anhydrous THF (5 mL) and cooled to 0°C under a nitrogen atmosphere. To this mixture was added a solution of compound **26** (0.47 mmol, 0.19 g) in anhydrous THF (2.5 mL) and stirred for 15 minutes at 0°C. A solution of compound **24** (0.60 mmol, 0.15 g) in THF (1.2 mL) was added to the reaction mixture and stirred for 2 hours at 0°C. Then the mixture was heated to 50°C for 20 minutes after which TLC analysis (7% MeOH in DCM, R_f=0.5 (slightly below compound **26**)) indicated complete conversion of the starting material. H_2O (1.4 mmol, 25 µL) and 98% H_2SO_4 (1.1 mmol, 60 µL) were added and the mixture was stirred for 1 hour at reflux temperature. The mixture was poured in H_2O and washed with DCM (3x). The organic layers were combined, dried ($MgSO_4$) and concentrated *in vacuo*. Silica gel column chromatography (DCM→1% MeOH in DCM, Δ=0.25%) yielded the title compound (0.27 mmol, 0.15 g, 57%).**^{1}H NMR (400 MHz, $CDCl_3$)** δ = 3.77 – 3.57 (m, 44H), 3.39 (t, *J*=5.1, 2H), 3.01 (s, 2H). **^{13}C NMR (101 MHz, $CDCl_3$)** δ = 72.49, 70.57, 70.55, 70.52, 70.44, 70.40, 70.18, 69.93, 61.52, 50.55.

Compound 28

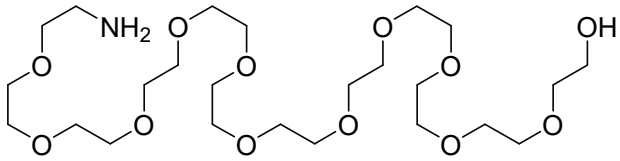

Compound **27** (0.27 mmol, 154 mg) was dissolved in anhydrous THF (2 mL) under an nitrogen atmosphere and cooled to 0°C. Triphenylphosphine (0.35 mmol, 0.091 mg) was added and the mixture was stirred for 18 hours at room temperature. H_2O (0.70 mmol, 13 µL) was added and the reaction was stirred for 48 hours. H_2O (7 mL) was added and the white precipitate was removed by filtration. The water layer was washed with toluene (3x). The organic layers were discarded and the water layer was concentrated *in vacuo* to yield the title compound (0.20 mmol, 0.11 g, 74%). **^{1}H NMR (400 MHz, $CDCl_3$)** δ = 3.79 – 3.55 (m, 47H), 3.51 (t, *J*=5.2, 2H), 2.86 (t, *J*=5.2, 2H), 2.20 (s, 3H). **^{13}C NMR (101 MHz, $CDCl_3$)** δ = 73.27, 72.61, 70.54, 70.50, 70.28, 70.23, 61.46, 41.68.

Compound 29

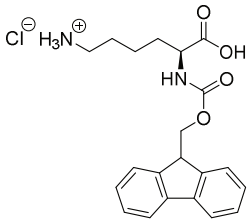

Fmoc-Lys(Boc)-OH (21.3 mmol, 10.0 g) was slowly added to dry 5M HCl in EA (150 mL). The solution was stirred for 30 min, after which the formed crash was isolated by filtration. The residue was washed with EA (3x) to yield the title compound (19.7 mmol, 7.98 g, 92%). **HRMS**: $[M+H]^+$ calculated for $C_{21}H_{25}N_2O_4$ 369.18088; found 369.18035 **IR(cm^{-1})=** 3320 (1° N-H, stretch), 2918 (O-H, stretch), 1690 (C=O, stretch)

Compound 30

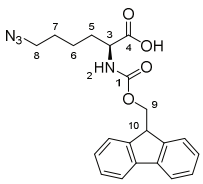

Compound **29** (19,7 mmol, 7,98 g) was dissolved in 8:2 MeOH:H_2O (150 mL). $CuSO_4$ (0.5 mmol, 80 mg), $NaHCO_3$ (90 mmol, 7.56 g) and HCl.imidazole-1-sulfonyl azide (0.5 mmol, 80 mg), $NaHCO_3$ (90 mmol, 7.56 g) and HCl.imidazole-1-sulfonyl azide (24 mmol, 5.0 g) was added. After overnight stirring, 3M HCl (aq) (30 mL) was added to acidify the solution to pH=2. The methanol was evaporated *in vacuo* and the mixture was diluted with EA and consequently washed with 10% $KHSO_4$ (aq) (3x) and brine (1x). The solution was dried ($MgSO_4$), filtrated and concentrated. The crude was adsorbed on Celite and purified by silica gel column chromatography (9:1 Pnt:EA → 5:5 Pnt:EA, Δ=5%) to yield the title compound (14.8 mmol, 5.84 g, 75%). **HRMS**: $[M+H]^+$ calculated for $C_{21}H_{22}N_4O_4$ 395.17138; found 395.17120 **IR(cm^{-1})=** 2949 (C-H, stretch), 2093 (N=N=N, stretch), 1694 (C=O, stretch). **^{1}H NMR (400 MHz, $CDCl_3$) δ** 9.38 (s, 1H, COOH), 7.74 (d, *J* = 7.5 Hz, 2H, C-H Fmoc), 7.59 (d, *J* = 5.8 Hz, 2H, C-H Fmoc), 7.38 (t, *J* = 7.4 Hz, 2H, C-H Fmoc), 7.29 (m, 2H, C-H Fmoc), 5.47 (d, *J* = 33.8 Hz, 1H, N_2), 4.51 (m, 1H, C_9), 4.39 (m, 2H, C_{3+9}), 4.20 (t, *J* = 6.8 Hz, 1H, C_{10}), 3.22 (m, 2H, C_8), 1.99 – 1.82 (m, 0.5H, C_5), 1.80 – 1.65 (m, 0.5H, C_5), 1.58 (m, 2H, C_6), 1.52 – 1.38 (m, 2H, C_7).**^{13}C NMR (101 MHz, $CDCl_3$) δ** 176.38 (C_4), 156.31 (C_1), 143.82 (C_q Fmoc), 141.35 (C_q Fmoc), 127.83 (C-H Fmoc), 127.15 (C-H Fmoc), 125.12 (C-H Fmoc), 120.09 (C-H Fmoc), 67.19 (C_9), 53.62 (C_3), 51.09 (C_8), 47.14 (C_{10}), 31.81 (C_5), 28.38 (C_6), 22.51 (C_7).

Structure of resin linker used (Rink amide)

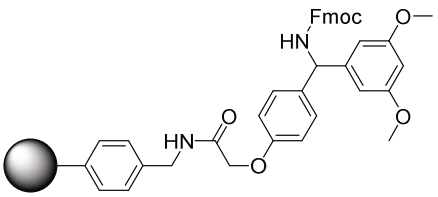

Rink amide resin(100-200 mesh, 0.7 mmole/g) was purchased from www.rapp-polymere.com.

Resin-bound compound 31

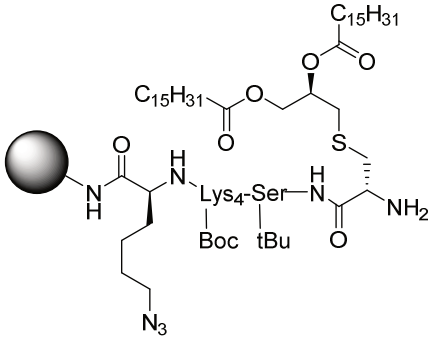

Rink amide resin (200 µmol) was treated with a solution of 20% piperidine in DMF (4x) for 10 min. and consequently washed with DMF (5x). This was followed by a coupling cycle procedure consisting of the following. The resin was treated with HCTU (1 mL, 0,6M in DMF), Fmoc-Cys(R-Pam_2)-OH (1mL, 0.6M in DMF) and lastly DiPEA (1mL, 0.6M in DMF). The reaction was shaken for 2 hours and consequently washed with DMF (5x). A solution of 5% acetic anhydride in 0.1M DiPEA in DMF was added and the syringe was shaken for 10 min. The resin was washed with DMF (5x) after which the resin was treated with a solution of 20% piperidine in DMF (4x) for 10 min. and consequently washed with DMF (5x).The coupling cycle was then started over by coupling the next amino acid. The first amino acid used in the coupling cycle was compound **30**. The last amino acid used in the coupling cycle was compound **5**.

Compound 32

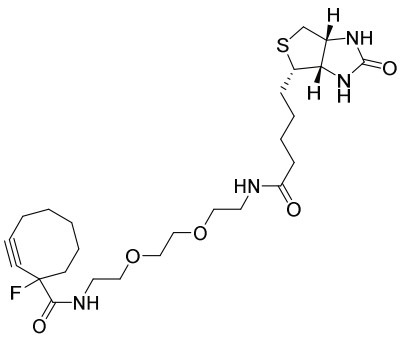

Compound **32** was synthesized in-house[30] via a literature procedure.[31]

Compound 33

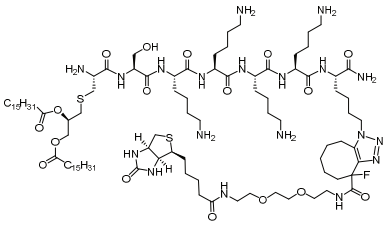

Resin-bound compound **31** (48 mg, 10 µmol) was swollen in a reaction syringe in DCM for 1 hour. Excess solvent was removed after which a solution of 95% TFA, 2.5% H_2O, 2.5% TIS was added. The reaction syringe was shaken for 2 hours after which the syringe was emptied in a tube containing cold diethyl ether. The tube was centrifuged to collect the

precipitation as a pellet suspended in diethyl ether. The pellet was dried over nitrogen gas and consequently dissolved in DMSO (1 mL). Of this solution 900 µL was taken and put in an Eppendorf tube. Compound **32** (4.7 mg, 9 µmol) was added and the tube was shaken over 3 days when LC-MS showed complete conversion of the peptide starting material. The crude was purified by reverse-phase HPLC (Gradient: 10% AcN + 90% (H_2O+0.1% TFA) to 90% AcN + 10% (H_2O+0.1% TFA)) to obtain compound **33** (0.20 µmol, 0.39 mg, 2%) **HRMS**: $[M+2H]^{2+}$ calculated for $C_{96}H_{178}FN_{19}O_{17}S_2$ 976.6552; found 976.6570

Compound 34

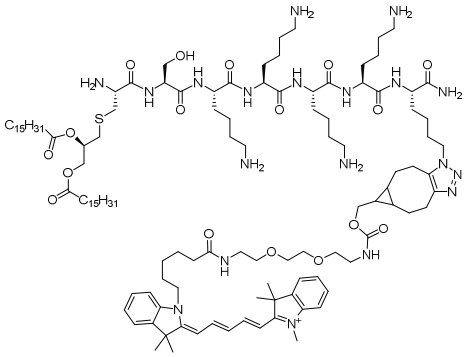

Resin-bound compound **31** (48 mg, 10 µmol) was swollen in a reaction syringe in DCM for 1 hour. Excess solvent was removed after which a solution of 95% TFA, 2.5% H_2O, 2.5% TIS was added. The reaction syringe was shaken for 2 hours after which the syringe was emptied in a tube containing cold diethyl ether. The tube was centrifuged to collect the precipitation as a pellet suspended in diethyl ether. The pellet was dried over nitrogen gas and consequently dissolved in DMSO (1 mL). Of this solution, 100 µL was put in an Eppendorf tube (1.5 mL). BCN-Cy5 (1 µmol, 0.81 mg) was added and the tube was shaken for 3 days at room temperature. LC-MS analysis indicated complete conversion of the starting material. The crude was purified by reverse-phase HPLC to yield the title compound (0.20 µmol, 0.44 mg, 20% overall yield) **LC-MS (1090, C18, H_2O/AcN + TFA):** 1107.27 (z=2, simulated), 1107.73 (z=2, observed), 1164.13 (z=2, TFA adduct), 1221.00 (z=2, 2*TFA adduct), 1277.53 (z=2, 3*TFA adduct). **HRMS**: $[M+3H]^{4+}$ calculated for $C_{120}H_{205}N_{19}O_{17}S$ 554.38726; found 554.38633

Compound 35

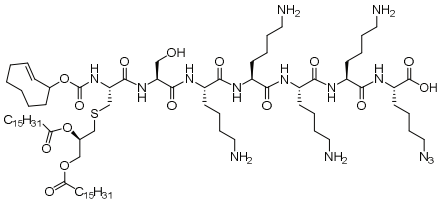

Resin-bound compound **31** (40 mg, 10 µmol) was swollen in DMF and DiPEA (50 µmol, 9 µL) and TCO-OSu (50 µmol, 13 mg) were added and the reaction syringe was shaken overnight. LC-MS analysis of a small amount of TFA-treated resin indicated complete conversion of the starting material. The resin was washed with DMF (3x) and DCM (3x). A solution of 5% TFA, 2.5% TIS, 2.5% H_2O in DCM was added and the reaction vessel was shaken for 15 min. The syringe was emptied in a 0°C solution of Et_2O (total volume = 30 mL) and put in a -20°C freezer overnight. The tube was then centrifuged for 90 min at 4°C after which a pellet was visible. The tube was decanted and the pellet dried to yield the title compound (2.3 µmol, 3.3 mg, 23%).

Compound 36

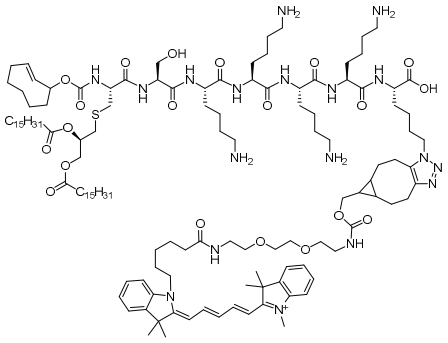

A solution of compound **35** (max. 2.3 µmol, 3.3 mg) in anhydrous DMSO (200 µL) was put in an Eppendorf tube (1.5 mL). BCN-Cy5 (1.1 µmol, 0.90 mg) was added and the tube was shaken for 3 days at room temperature. LC-MS analysis indicated complete conversion of the starting material. The mixture was diluted with DMSO (500 µL) and a mixture of 1:1:1 *t*-BuOH:AcN:H_2O (500 µL). The crude was purified by reverse-phase HPLC to yield the title compound (0.60 µmol, 1.4 mg, 26% overall yield). **HRMS**: $[M+3H]^{3+}$ calculated for $C_{129}H_{215}N_{18}O_{20}S$ 789.86993; found 789.86841

References

(1) van de Graaff, M. J.; Oosenbrug, T.; Marqvorsen, M. H. S.; Nascimento, C. R.; de Geus, M. A. R.; Manoury, B.; Ressing, M. E.; van Kasteren, S. I. Conditionally Controlling Human TLR2 Activity via Trans-Cyclooctene Caged Ligands. *Bioconjugate Chem.* **2020**, *31* (6), 1685–1692.

(2) Oosenbrug, T.; van de Graaff, M. J.; Haks, M. C.; van Kasteren, S.; Ressing, M. E. An Alternative Model for Type I Interferon Induction Downstream of Human TLR2. *J. Biol. Chem.* **2020**, *295* (42), 14325–14342.

(3) Flo, T. H.; Halaas, Ø.; Torp, S.; Ryan, L.; Lien, E.; Dybdahl, B.; Sundan, A.; Espevik, T. Differential Expression of Toll-like Receptor 2 in Human Cells. *J. Leukoc. Biol.* **2001**, *69* (3), 474–481.

(4) Kang, J. Y.; Nan, X.; Jin, M. S.; Youn, S.-J.; Ryu, Y. H.; Mah, S.; Han, S. H.; Lee, H.; Paik, S.-G.; Lee, J.-O. Recognition of Lipopeptide Patterns by Toll-like Receptor 2-Toll-like Receptor 6 Heterodimer. *Immunity* **2009**, *31* (6), 873–884.

(5) Jin, M. S.; Kim, S. E.; Heo, J. Y.; Lee, M. E.; Kim, H. M.; Paik, S.-G.; Lee, H.; Lee, J.-O. Crystal Structure of the TLR1-TLR2 Heterodimer Induced by Binding of a Tri-Acylated Lipopeptide. *Cell* **2007**, *130* (6), 1071–1082.

(6) Aliprantis, A. O. Cell Activation and Apoptosis by Bacterial Lipoproteins Through Toll-like Receptor-2. *Science* **1999**, *285* (5428), 736–739.

(7) Kagan, J. C.; Su, T.; Horng, T.; Chow, A.; Akira, S.; Medzhitov, R. TRAM Couples Endocytosis of Toll-like Receptor 4 to the Induction of Interferon-β. *Nat Immunol* **2008**, *9* (4), 361–368.

(8) Tatematsu, M.; Yoshida, R.; Morioka, Y.; Ishii, N.; Funami, K.; Watanabe, A.; Saeki, K.; Seya, T.; Matsumoto, M. Raftlin Controls Lipopolysaccharide-Induced TLR4 Internalization and TICAM-1 Signaling in a Cell Type–Specific Manner. *J.I.* **2016**, *196* (9), 3865–3876.

(9) Lu, Y.-C.; Yeh, W.-C.; Ohashi, P. S. LPS/TLR4 Signal Transduction Pathway. *Cytokine* **2008**, *42* (2), 145–151.

(10) Dutta, D.; Donaldson, J. G. Search for Inhibitors of Endocytosis: Intended Specificity and Unintended Consequences. *Cellular Logistics* **2012**, *2* (4), 203–208.

(11) Mancini, R. J.; Stutts, L.; Moore, T.; Esser-Kahn, A. P. Controlling the Origins of Inflammation with a Photoactive Lipopeptide Immunopotentiator. *Angew. Chem. Int. Ed.* **2015**, *54* (20), 5962–5965.

(12) Ryu, K. A.; Stutts, L.; Tom, J. K.; Mancini, R. J.; Esser-Kahn, A. P. Stimulation of Innate Immune Cells by Light-Activated TLR7/8 Agonists. *J. Am. Chem. Soc.* **2014**, *136* (31), 10823–10825.

(13) Denk, W. Two-Photon Scanning Photochemical Microscopy: Mapping Ligand-Gated Ion Channel Distributions. *Proceedings of the National Academy of Sciences* **1994**, *91* (14), 6629–6633.

(14) Lee, R. E. C.; Walker, S. R.; Savery, K.; Frank, D. A.; Gaudet, S. Fold Change of Nuclear NF-KB Determines TNF-Induced Transcription in Single Cells. *Molecular Cell* **2014**, *53* (6), 867–879.

(15) Lee, T. K.; Denny, E. M.; Sanghvi, J. C.; Gaston, J. E.; Maynard, N. D.; Hughey, J. J.; Covert, M. W. A Noisy Paracrine Signal Determines the Cellular NF-KB Response to Lipopolysaccharide. *Science Signaling*, **2009**, *2* (93), ra65.

(16) Blackman, M. L.; Royzen, M.; Fox, J. M. Tetrazine Ligation: Fast Bioconjugation Based on Inverse-Electron-Demand Diels–Alder Reactivity. *J. Am. Chem. Soc.* **2008**, *130* (41), 13518–13519.

(17) Versteegen, R. M.; Rossin, R.; ten Hoeve, W.; Janssen, H. M.; Robillard, M. S. Click to Release: Instantaneous Doxorubicin Elimination upon Tetrazine Ligation. *Angew. Chem. Int. Ed.* **2013**, *52* (52), 14112–14116.

(18) van der Gracht, A. M. F.; de Geus, M. A. R.; Camps, M. G. M.; Ruckwardt, T. J.; Sarris, A. J. C.; Bremmers, J.; Maurits, E.; Pawlak, J. B.; Posthoorn, M. M.; Bonger, K. M.; Filippov, D. V.; Overkleeft, H. S.; Robillard, M. S.; Ossendorp, F.; van Kasteren, S. I. Chemical Control over T-Cell Activation *in Vivo* Using Deprotection of *Trans* -Cyclooctene-Modified Epitopes. *ACS Chem. Biol.* **2018**, *13* (6), 1569–1576.

(19) Rossin, R.; Versteegen, R. M.; Wu, J.; Khasanov, A.; Wessels, H. J.; Steenbergen, E. J.; ten Hoeve, W.; Janssen, H. M.; van Onzen, A. H. A. M.; Hudson, P. J.; Robillard, M. S. Chemically Triggered Drug Release from an Antibody-Drug Conjugate Leads to Potent Antitumour Activity in Mice. *Nat Commun* **2018**, *9* (1), 1484.

(20) Fan, X.; Ge, Y.; Lin, F.; Yang, Y.; Zhang, G.; Ngai, W. S. C.; Lin, Z.; Zheng, S.; Wang, J.; Zhao, J.; Li, J.; Chen, P. R. Optimized Tetrazine Derivatives for Rapid Bioorthogonal Decaging in Living Cells. *Angew. Chem. Int. Ed.* **2016**, *55* (45), 14046–14050.

(21) Sarris, A. J. C.; Hansen, T.; de Geus, M. A. R.; Maurits, E.; Doelman, W.; Overkleeft, H. S.; Codée, J. D. C.; Filippov, D. V.; van Kasteren, S. I. Fast and PH-Independent Elimination of *Trans* -Cyclooctene by Using Aminoethyl-Functionalized Tetrazines. *Chem. Eur. J.* **2018**, *24* (68), 18075–18081.

(22) Omueti, K. O.; Beyer, J. M.; Johnson, C. M.; Lyle, E. A.; Tapping, R. I. Domain Exchange between Human Toll-like Receptors 1 and 6 Reveals a Region Required for Lipopeptide Discrimination. *J. Biol. Chem.* **2005**, *280* (44), 36616–36625.

(23) Metzger, J. W.; Wiesmüller, K.-H.; Jung, G. Synthesis of Nα-Fmoc Protected Derivatives of S-(2,3-Dihydroxypropyl)-Cysteine and Their Application in Peptide Synthesis. *International Journal of Peptide and Protein Research* **2009**, *38* (6), 545–554.

(24) El Oualid, F.; Merkx, R.; Ekkebus, R.; Hameed, D. S.; Smit, J. J.; de Jong, A.; Hilkmann, H.; Sixma, T. K.; Ovaa, H. Chemical Synthesis of Ubiquitin, Ubiquitin-Based Probes, and Diubiquitin. *Angew. Chem. Int. Ed.* **2010**, *49* (52), 10149–10153.

(25) Rossin, R.; van Duijnhoven, S. M. J.; ten Hoeve, W.; Janssen, H. M.; Kleijn, L. H. J.; Hoeben, F. J. M.; Versteegen, R. M.; Robillard, M. S. Triggered Drug Release from an Antibody–Drug Conjugate Using Fast "Click-to-Release" Chemistry in Mice. *Bioconjugate Chem.* **2016**, *27* (7), 1697–1706.

(26) Wilkinson, B. L.; Day, S.; Malins, L. R.; Apostolopoulos, V.; Payne, R. J. Self-Adjuvanting Multicomponent Cancer Vaccine Candidates Combining Per-Glycosylated MUC1 Glycopeptides and the Toll-like Receptor 2 Agonist Pam3CysSer. *Angew. Chem. Int. Ed.* **2011**, *50* (7), 1635–1639.

(27) Zhang, H.; Li, X.; Shi, Q.; Li, Y.; Xia, G.; Chen, L.; Yang, Z.; Jiang, Z.-X. Highly Efficient Synthesis of Monodisperse Poly(Ethylene Glycols) and Derivatives through Macrocyclization of Oligo(Ethylene Glycols). *Angew. Chem. Int. Ed.* **2015**, *54* (12), 3763–3767.

(28) Versteegen, R. M.; ten Hoeve, W.; Rossin, R.; de Geus, M. A. R.; Janssen, H. M.; Robillard, M. S. Click-to-Release from *Trans* -Cyclooctenes: Mechanistic Insights and

Expansion of Scope from Established Carbamate to Remarkable Ether Cleavage. *Angew. Chem. Int. Ed.* **2018**, *57* (33), 10494–10499.

(29) de Geus, M. A. R.; Groenewold, G. J. M.; Maurits, E.; Araman, C.; van Kasteren, S. I. Synthetic Methodology towards Allylic *Trans* -Cyclooctene-Ethers Enables Modification of Carbohydrates: Bioorthogonal Manipulation of the *Lac* Repressor. *Chem. Sci.* **2020**, *11* (37), 10175–10179.

(30) Van Der Linden, W. A.; Li, N.; Hoogendoorn, S.; Ruben, M.; Verdoes, M.; Guo, J.; Boons, G. J.; Van Der Marel, G. A.; Florea, B. I.; Overkleeft, H. S. Two-Step Bioorthogonal Activity-Based Proteasome Profiling Using Copper-Free Click Reagents: A Comparative Study. *Bioorganic and Medicinal Chemistry* **2012**, *20* (2), 662–666.

(31) Schultz, M. K.; Parameswarappa, S. G.; Pigge, F. C. Synthesis of a DOTA-Biotin Conjugate for Radionuclide Chelation via Cu-Free Click Chemistry. *Organic Letters* **2010**, *12* (10), 2398–2401.